NASA Technical Memorandum 83465

A Review of Liquid Lubricant Thermal/Oxidative Degradation

William R. Jones, Jr.
Lewis Research Center
Cleveland, Ohio

August 1983

NASA

A REVIEW OF LIQUID LUBRICANT THERMAL/OXIDATIVE DEGRADATION

William R. Jones, Jr.
National Aeronautics and Space Administration
Lewis Research Center
Cleveland, Ohio 44135

ABSTRACT

The fundamental processes occurring during the thermal and oxidative degradation of hydrocarbons are reviewed. Particular emphasis is given to various classes of liquid lubricants such as mineral oils, esters, polyphenyl ethers, C-ethers, and fluorinated polyethers. Experimental techniques for determining thermal and oxidative stabilities of lubricants are discussed. The role of inhibitors and catalysis is also covered.

INTRODUCTION

Liquid lubricants are being subjected to ever-increasing thermal stresses. The role of the lubricants thermal and oxidative stabilities is becoming an important factor in their survivability at high temperatures in oxidizing environments. Maximum fluid temperatures have been estimated to be in excess of 260° C for many applications (refs. 1 to 8).

State-of-the-art fluids (esters, hydrocarbons, silicones, fluorinated polyethers, C-ethers, and polyphenyl ethers) have one or more deficiencies which limit or prevent their performance above 260° C. Some of these deficiencies are related to physical properties such as pour point or volatility, but for many the chemical stability at these high temperatures is the weak link.

The objective of this paper is to review the fundamentals of thermal and oxidative breakdown processes occurring in liquid lubricants. In addition, the probable mechanisms of lubricant breakdown are reviewed for several chemical classes (hydrocarbons, esters, C-ethers, polyphenyl ethers, and fluorinated polyethers).

THERMAL STABILITY

It is unfortunate that the literature is often not explicit concerning the term "thermal stability". It is sometimes used interchangeably with thermal-oxidative stability. However, the proper definition is reserved for processes occurring in the absence of oxygen.

Mechanism

In the case of hydrocarbons and most other fluid classes, thermal decomposition or pyrolysis proceeds through a free-radical chain reaction process yielding many products. Free radicals are organic fragments containing an unpaired electron. These radicals are produced by homolysis (breaking) of C-C

bonds. These radicals can be generated by radiation, mechanical processes, and thermal energy (ref. 9).

The production of free radicals from a hydrocarbon by a thermal process (refs. 10 and 11) is illustrated in equation (1)

$$R\text{-}CH_2\text{-}CH_3 \rightarrow R\bullet + R\text{-}CH_2\text{-}\dot{C}H_2 + R\text{-}\dot{C}H\text{-}CH_3 \qquad (1)$$

These radicals are highly reactive and start reaction chains by abstracting hydrogen atoms (H) from the parent hydrocarbon. The chainlike reaction arises from a simple mathematical principle - the sum of an even plus an odd number is always an odd number. When a radical (odd number of electrons) attacks a nonradical (even number of electrons) one of the resulting species must have an odd number of electrons. Therefore, it is a radical itself and also capable of attacking a nonradical. Attack by this second radical (possibly different than the initial radical) will produce a third radical. Abstraction reactions are illustrated in equation (2)

$$R\bullet + R\text{-}CH_2\text{-}CH_3 \longrightarrow RH + R\text{-}CH_2\text{-}\dot{C}H_2 \qquad (2)$$
$$\searrow \quad RH + R\text{-}\dot{C}H\text{-}CH_3$$

This chain sequence will continue until the radicals are destroyed or all of the reactants are consumed. Hence, a single radical can bring about changes in thousands of molecules. Radicals may be destroyed by recombination (eq. (3))

$$R\bullet + R\bullet \rightarrow R\text{-}R \qquad (3)$$

or through disproportionation reactions (transfer of an atom from one radical to another) as in equation (4).

$$R\bullet + H\text{-}CH_2\text{-}\dot{C}H_2 \rightarrow RH + CH_2 = CH_2 \qquad (4)$$

Radicals themselves may also fragment producing new radicals and unsaturated species (eq. (5)).

$$R\text{-}CH_2\text{-}\dot{C}H_2 \rightarrow R\bullet + CH_2 = CH_2 \qquad (5)$$

These reactions occur in industrial "cracking".

Although higher molecular weight products may be produced in this series of reactions, the most general change in properties of the lubricant is an increase in the vapor pressure of the system. This is brought about by cleavage of large molecules into smaller, more volatile, gaseous fragments. This gaseous evolution can be utilized to quantitate the thermal stability of organic compounds.

Arrhenius Rate Law

The rate of thermal decomposition usually varies with temperature according to the empirical Arrhenius rate law (ref. 12) as shown in the following equation:

$$k = Ae^{-E/RT} \tag{6}$$

where k is the rate constant, A is the frequency factor or preexponential factor, E is the activation energy, R the gas constant, and T the absolute temperature. According to this equation, a straight line should be obtained when $\log k$ is plotted as a function of the reciprocal of the absolute temperature. It has been shown (ref. 12) that for most organic compounds $\log dp/dt$ versus $1/T$ is also a straight line. Then, by analogy,

$$\frac{dp}{dt} = A'e^{-E'/RT} \tag{7}$$

Using this equation, one can define the rate constant for thermal decomposition by measuring the isothermal rate of vapor pressure rise at several temperatures. However, it is more convenient to have a single parameter for thermal decomposition rather than to tabulate values of A' and E' which actually define the rate constant.

Therefore, an arbitrary thermal decomposition temperature (T_D) is defined as the temperature at which the isothermal rate of vapor pressure rise is 1.85 Pa/sec (50 torr/hr). Then, the decomposition points for a series of organic compounds are the temperatures at which all have identical isothermal rates of vapor pressure rise. This is the technique used in the standard test method (ASTM D2879) (ref. 13) for measuring the initial decomposition temperature of liquids. This test uses a constant volume device (the isoteniscope) which can also be used to measure vapor pressure as a function of temperature.

Tensimeter

An automated device (the tensimeter), based on the same principle, (ref. 14) also yields thermal decomposition temperatures and vapor pressure data. A schematic representation of the tensimeter appears in figure 1. The sample cell is made of ordinary borosilicate glass and has a volume of about 5 ml (5×10^{-6} m^3). Three to four milliliters (3×10^{-6} to 4×10^{-6} m^3) of test fluid are placed in the sample cell. The sample is then degassed and refluxed under a vacuum. The cell is placed in a temperature-programmed oven and heated to an initial temperature about 50° C below the suspected decomposition temperature. After a 5-minute stabilization period, the increase in vapor pressure, if any, is recorded as a vertical bar during a fixed time interval. Then the programmer automatically raises the temperature by a preset amount (usually 5° C) and the same process is repeated. A typical thermal decomposition curve for a synthetic hydrocarbon is shown in figure 2. This is a plot of the logarithm of the isothermal rate of vapor pressure increase as a function of reciprocal absolute temperature. A straight line is drawn connecting the tops of the recorded bars. The intersection of this line with the temperature axis

is the T_D. In addition, the activation energy for decomposition (E') can be calculated from the slope of this line.

Useful Lives

From a knowledge of the T_D and E', a useful life of a lubricant (in the absence of oxygen) can be calculated from the following equation (ref. 12).

$$t = \frac{0.0285\ T_D}{MW} \log\left(\frac{100-x}{100}\right) \text{antilog}\left[5 - 219\ E'\left(\frac{1}{T_D} - \frac{1}{T}\right)\right] \qquad (8)$$

where t is time, MW is molecular weight, and x is the percent decomposition at temperature T. The useful life is typically defined as the time in hours required for 10 percent decomposition. A plot of useful lives for several lubricants appears in figure 3 (from ref. 15).

Generalizations

Blake et al. (ref. 12) reported on the thermal decomposition of a variety of different chemical structures. From their data and that of others (refs. 15 to 20) one can make the following generalizations:

(1) The maximum thermal stability of a straight chain hydrocarbon or other compounds containing such groups is about 350° C.

(2) Branched chain hydrocarbons are less stable than straight chain hydrocarbons due to steric effects and the fact that free radicals of greater stability are formed.

(3) However, steric crowding around larger central atoms such as tin and silicon actually increases the thermal stability compared to the less crowded tin and silicon compounds.

(4) Aromatic bonds (C-H and C-C) have higher dissociation energies due to resonance and therefore these compounds are much more stable than their aliphatic analogs. Maximum stabilities of this class approach 450° C.

(5) Esters of alcohols having β-hydrogens decompose through a low energy transition state with maximum T_D's near 280° C.

(6) Esters not containing β-hydrogens have the low energy reaction path blocked and therefore exhibit stabilites approaching hydrocarbons (320° to 340° C).

(7) Substitutions on an aromatic ring decrease its stability. Increasing the number of substituents continually decreases stability. Increasing the chain length also decreases stability until it approaches that of aliphatic hydrocarbons.

(8) Saturated ring compounds are more stable than their straight chain analogs.

(9) Completely replacing hydrogen with fluorine sometimes increases the thermal stability of an organic compound (some exceptions are aromatics and esters).

Bond Dissociation Energy

These generalizations arise from the fact that thermal decomposition occurs at the weakest link in the compound. Therefore, thermal decomposition should be a function of the weakest bond dissociation energy (E_{DIS}) in that compound. Table I tabulates T_D and E_{DIS} values for a variety of compounds. The thermal decomposition temperature is then plotted as a function of the bond dissociation energy in figure 4. Here the general trend of increasing T_D with increasing E_{DIS} is apparent.

Bond Length

Since bond length is inversely related to bond strength, it can also be correlated with thermal decomposition temperature. Figure 5 contains a plot of T_D versus the reciprocal of bond length for a series of aromatic compounds of the type $(C_6H_5)_nM$ where M is a Group V element. Here the correlation is much better than in figure 4 since the compounds are structurally very similar except for the central atom.

Degradation Products

In general, two types of thermal degradation are observed with organic fluids. One type is random degradation in which a great number of decomposition products are produced. A saturated straight chain hydrocarbon is an example. A second type is called chain depolymerization (or unzipping). Here the compound reverts to its monomer. Polyolefin fluids are examples. Polymers have analogous decomposition routes with polytetrafluoroethylene behaving in an unzipping mode while polyethylene exhibits a random degradation or chain scission (ref. 21). Both processes proceed by free radical mechanisms.

Many fluids, however, exhibit a combination of these mechanisms. Two factors that are important for chain depolymerization to occur are:

(1) The reactivity of the depropagating radical
(2) The availability of a reactive hydrogen atom which could allow chain transfer.

For example, all polymers having α-hydrogens (such as polyacrylates) yield little monomer. On the other hand, polymers such as polymethacrylates give high yields of monomer because of the blocking action of the α-methyl group. Polytetrafluoroethylene also depolymerizes due to the resistance of the C-F bonds to chain transfer.

Catalytic Thermal Decomposition

Blake et al. (ref. 12) has reported that the thermal stability of most chemical classes is not affected by the presence of metal surfaces. One exception is esters, which yield decreases in T_D from 35° to 60° C in the presence of steel (ref. 12) or iron powder (ref. 15). Klaus has also shown that a number of hydrocarbons were not affected by the presence of various catalyst coupons (ref. 20). However, recent work (ref. 22) with two esters (DES and TMPTH) has yielded interesting results in evaporation tests in nitrogen. At temperatures below 180° C, evaporation losses are unaffected by

metals. However, above 180° C, the rate of evaporation is increased and is different for different metals. This effect is shown in figure 6 (ref. 22). This suggests that thermal degradation is being catalyzed by the metals yielding lower MW products which increase the evaporation rate.

Effect of Additives on Thermal Stability

There are many additives that are effective in increasing the oxidation stability of lubricants which will be discussed later. However, additives do not normally affect thermal stability of the base fluid. This was confirmed by evaporation tests using a formulated ester containing phenothiazine (PTZ), a phenyl-α-naphylamine (PANA), and tricresylphosphate (TCP). No differences were noted compared to the nonadditive fluid (ref. 22).

OXIDATION STABILITY

The oxidation of an organic compound with molecular oxygen is usually referred to as autoxidation. As was the case with thermal decomposition, oxidation usually proceeds through a free radical chain mechanism (ref. 23). However, with the additional participant (oxygen) the reactions can become exceedingly complex. The importance of hydroperoxides in the oxidation process was shown by Criegee (ref. 24).

Mechanism

The liquid-phase oxidation of organic compounds and liquid lubricants has been studied by many investigators (refs. 25 to 56). In general, the basic mechanism is thought to proceed as follows (ref. 57).

$$In_2 \xrightarrow{R_i} 2\ In\bullet \qquad \text{Initiation} \qquad (9)$$

$$In\bullet + RH \rightarrow InH + R\bullet \qquad (10)$$

Here an initiator (In) produces free radicals (In•) at reaction rate (R_i) which abstracts a proton from the hydrocarbon and produces an alkyl free radical (R•). This highly reactive species reacts with oxygen in the propagation step of the chain reaction:

$$R\bullet + O_2 \rightarrow RO_2\bullet \qquad \text{Propagation} \qquad (11)$$

This propagation step produces a peroxy radical (RO_2•) which, in turn, reacts with the parent hydrocarbon (RH) to produce a hydroperoxide (RO_2H).

$$RO_2\bullet + RH \xrightarrow{k_p} RO_2H + R\bullet \qquad (12)$$

This reaction regenerates a alkyl free radical (R•) which propagates the chain.

The chain reaction can be terminated by radical coupling of two peroxy radicals (RO_2•).

$$2RO_2\bullet \xrightarrow{2k_t} RO_4R \qquad \text{nonradical products} \tag{13}$$

or by cross termination of an alkyl radical (R•) and a peroxyradical (RO_2•).

$$R\bullet + RO_2\bullet \rightarrow RO_2R \tag{14}$$

The third possibility is the termination reaction of two alkyl radicals (R•).

$$2R\bullet \rightarrow R\text{-}R \tag{15}$$

Rate Equations

For normal oxygen concentrations where $[RO_2\bullet] \gg R\bullet$, reactions (14) and (15) can be neglected. Therefore, the rate of oxidation of hydrocarbon R-H can be expressed as:

$$\frac{-d[R\text{-}H]}{dt} = k_p[R\text{-}H]\left(\frac{R_i}{2k_t}\right)^{1/2} \tag{16}$$

The rate of oxidation is then directly proportional to the hydrocarbon concentration and the square root of the rate of chain initiation. This relationship is illustrated in figure 7, which shows the rate of oxidation of ethyl linoleate (initiated by benzoyl peroxide) as a function of its concentration. For other types of chain termination, different rate of consumption equations will be obtained. Some of these relationships appear in reference 58.

Oxidizability

The ratio $k_p/(2k_t)^{1/2}$ which appears in equation (16) is referred to as the oxidizability. For a specific rate of initiation, the autoxidation of a hydrocarbon (R-H) is then determined by the values of k_p and k_t. The rate of chain propagation (k_p) can be estimated if the bond energy for the weakest C-H bond is known (ref. 59). The termination rate constant k_t can also be estimated. Thus, in theory, the oxidizability should be predictable for any pure hydrocarbon. Table II (ref. 60) contains a list of oxidizabilities for various hydrocarbons. This list illustrates the wide range of oxidation rates for different hydrocarbon structures.

However, this simple relationship (eq. (16)) breaks down at high conversions (>20 percent). Complications are caused by the accumulation and reaction of secondary products such as aldehydes and ketones.

Chain Initiation

As mentioned earlier, chain initiation can be effected by the deliberate addition of an initiator. Typical initiators are azo compounds and peroxides. This circumvents the long and sometimes irreproducible induction periods (time before oxygen absorption begins).

Initiation can also take place by direct reaction with oxygen:

$$RH + O_2 \rightarrow R\bullet + HO_2\bullet \qquad (17)$$

However, this reaction is thermodynamically and kinetically unfavorable. Initiation in the absence of added initiators is probably due to peroxidic impurities.

However, a common source of free radicals is the thermal decomposition of the alkyl hydroperoxides, producing an alkoxy and a hydroxy radical:

$$RO_2H \rightarrow RO\bullet + \bullet OH \qquad (18)$$

producing an alkoxy and a hydroxy radical. These radicals can then react with the parent hydrocarbon (RH).

$$RO\bullet + RH \rightarrow ROH + R\bullet \qquad (19)$$

$$\bullet OH + RH \rightarrow HOH + R\bullet \qquad (20)$$

producing water, alcohols, and alkyl radicals. These reactions are referred to as chain branching.

Chain Propagation

As indicated, the reaction of an alkyl radical (R•) and O_2 (in itself a biradical) proceeds very rapidly. The rate controlling step is then hydrogen abstraction by the alkylperoxy radical in equation (12).

The alkylperoxy radicals ($RO_2\bullet$) are more stable than the alkyl radicals (R•). They are quite persistent and selective. They preferentially abstract only the most labile hydrogen atom (weakest C-H bond). A group of H-bond energies appears in Table III (ref. 57). It is obvious that phenols, thiols, aromatic amines, and phosphines have the most labile hydrogen atoms. It is also clear that the relative attack for primary, secondary, and tertiary bonds should be in the order: tertiary (90 kcal) > secondary (94 kcal) > primary (103 kcal). Indeed, this has been shown to be the case for 2-methylpentane where the order is 300:30:1 (ref. 61), for tertiary, secondary, and primary bonds, respectively.

The propagation rate is also dependent on the type of hydrogen abstracting alkylperoxy radical. In order to correlate rates with C-H bond energies, rate constants for a series of hydrocarbons (R-H) should be compared for the same

alkylperoxy radical. Table IV (ref. 57) shows rate constants for a series of hydrocarbons against their own peroxy radicals (k_p) and against t-butylperoxy radicals (k_p). Obviously, reactivities are very structurally dependent. For example, the benzoylperoxy radical is 40 000 times more reactive than the t-butylperoxy radical toward benzaldehyde. Comparing only C-H bond energies (Table III) would lead one to conclude that aldehydes and alkylaromatic compounds would oxidize at similar rates. However, aldehydes oxidize at appreciably greater rates than the alkylaromatics due to the strong electron withdrawing effect of the carbonyl group.

Chain Termination

As previously mentioned, the normal termination reaction is

$$2RO_2\bullet \rightarrow RO_4R \qquad (13)$$

which is a tetroxide.

The decomposition of tetroxides is also highly dependent on the nature of the R-group. For example, secondary and primary alkylperoxy radicals undergo disproportionation to an alcohol and a ketone.

$$RO_4R \rightarrow R_2CO + R_2CHOH + O_2 \qquad (21)$$

Tert-alkylperoxy radicals yield a different mechanism resulting in the formation of dialkyl peroxides and O_2. The dialkyl peroxides undergo further decomposition. Therefore, primary and secondary alkylperoxy radicals yield much higher termination rates than tert-alkylperoxy radicals.

The oxidation rate of a hydrocarbon is determined by both the propagation rate (k_p) and the termination rate (k_t) as indicated in equation (16). This illustrates why a reactive hydrocarbon such as toluene ($C_6H_5-CH_2-H$), which has a C-H dissociation energy of only 85 kcal/mole, has a rather low autoxidation rate. This is due to the high termination rate of its primary alkylperoxy radicals.

Inhibition of Autoxidation

Autoxidations can be inhibited by the addition of scavengers which break the chain reaction by forming stable free radicals:

$$RO_2\bullet + XH \rightarrow RO_2H + X\bullet \qquad (22)$$

An example is in the use of substituted phenols (2,6-di-t-butyl-4-methylphenol) that would yield stable phenoxyl radicals (ArO•) which are far less reactive than the RO_2• radical or the R• normally formed by hydrogen abstraction from the parent hydrocarbon.

A second type of inhibitor causes the destruction of hydroperoxides (RO_2H). Here the inhibitor (X) reacts with the hydroperoxide (RO_2H) yielding nonradical products.

$$RO_2H + X \rightarrow ROH + XO \qquad (23)$$

An example of this type of inhibitor is phenothiazine (PTZ).

Metal coaters (such as tricresylphosphate) can sometimes be considered as a third type of inhibitor. Here their action is to prevent catalytic effects by coating metal surfaces.

The effectiveness of a chain breaking inhibitor is dependent on two factors (1) the reactivity or stability of the radical (X) formed from the inhibitor (X) and (2) the reaction rate of the peroxy radicals ($RO_2\bullet$) with the inhibitor (X). The reactivity of X is determined by the ratio of k_p/k_{24} of the following:

$$RO_2\bullet + RH \xrightarrow{k_p} RO_2H + R\bullet \qquad (12)$$

$$RH + X\bullet \xrightarrow{k_{24}} XH + R\bullet \qquad (24)$$

The lower this ratio, the greater the inhibition of the additive., If X• are completely inactive, k_p/k_{24} is very small and X is an excellent inhibitor. If X• is still capable of chain propagation, the chain reaction proceeds but at a lower rate.

The inhibitors effectiveness is also a function of its rate of reaction with peroxy radicals (k_{22}

$$RO_2\bullet + XH \xrightarrow{k_{22}} RO_2H + X\bullet \qquad (22)$$

The higher this rate (k_{22}) the lower the concentration of inhibitor required to decrease the rate of oxidation by a certain factor. The effectiveness may be defined as k_{22}/k_s where k_s is the reaction rate for some inhibitor in reaction 22 taken as a standard. Table V (ref. 25) shows the effectiveness for several phenols.

Metal Catalysis in Oxidation

Metal catalyzed oxidations are either homolytic (one electron processes) or heterolytic (two electron processes). Homolytic catalysis usually involves soluble transiton metal salts (homogeneous) such as napthanates of Co, Mn, Fe, and Cu, or the metal oxides (heterogeneous). Homolytic catalysis requires recyling of the metal species between several oxidation states by one electron

change. In addition, free radicals are produced during this mechanism. An example of this type of catalysis is illustrated in the following equations.

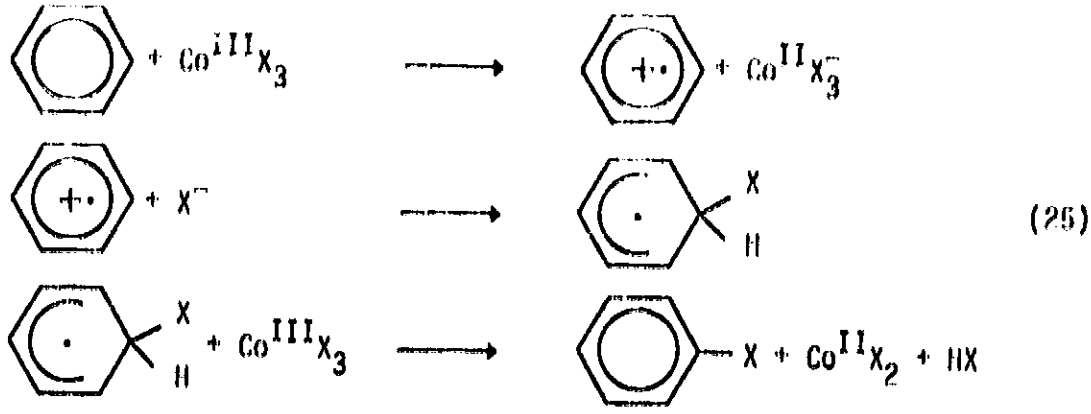

(25)

Although this is an oxidative substitution it does illustrate the homolytic process (i.e., the formation of free radicals and one electron transfer.

In constrast, heterolytic catalysis involves reactions of compounds coordinated to transition metals. The metal complex acts as a Lewis acid and undergoes two-equivalent changes. Free radicals are not involved. An example of this mechanism is shown here for another oxidative substitution.

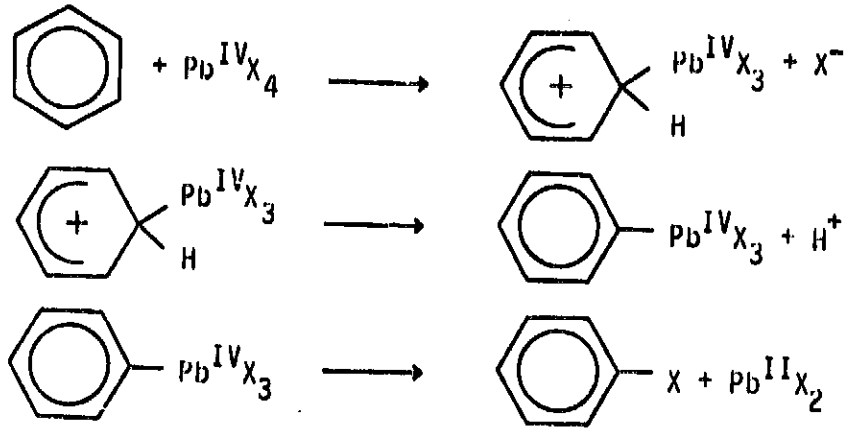

(26)

Catalysis of liquid phase autoxidations often proceed by homolytic decomposition of alkyl hydroperoxides. The rapid decomposition of these hydroperoxides in solutions containing iron, manganese, cobalt, and copper compounds is well known. The two basic reations are:

$$RO_2H + M^{(n-1)+} \rightarrow RO\cdot + M^{n+} + HO^- \qquad (27)$$

$$RO_2H + M^{n+} \rightarrow RO_2\cdot + M^{(n-1)+} + H^+ \qquad (28)$$

Therefore, metal complexes catalyze autoxidations by generating chain initiating radicals (eqs. (27) and (28)). In addition alkyl radicals (R·) may be produced directly from the parent hydrocarbon.

$$RH + M^{n+} \rightarrow R\bullet + H^{+} + M^{(n+1)+} \quad (29)$$

$$M^{n+} + O_2 \rightarrow M^{(n+1)} + O_2^{-}\bullet \quad (30)$$

Homogeneous and Heterogeneous Catalysis

The fundamental chemical processes occurring during oxidation are the same whether the process takes place in the coordination sphere of a soluble metal complex (homogeneous) or at an adsorabate-metal interface. The same mechanistic pathways are available to both kinds of catalysis. The local chemical structure of the active site is more important than the macroscopic features of a system, such as its physical state.

Chain Branching

From the introductory material it might appear that, at least for pure component systems, predictions of reaction rates and product distributions should be relatively easy to make. At sufficiently low temperatures (<100° C) and low conversions (<10 percent) this is probably true for many simple hydrocarbon systems.

Above 100° C there is an increasing tendency for the primary oxidation products (alkylhydroperoxides) (RO_2H) to decompose homolytically into alkoxy and hydroxy radicals as previously shown:

$$RO_2H \rightarrow RO\bullet + \bullet OH \quad (18)$$

These reactive species can further react with the parent hydrocarbon RH to produce more alkyl radicals.

$$RO\bullet + RH \rightarrow ROH + R\bullet \quad (19)$$

$$\bullet OH + RH \rightarrow HOH + R\bullet \quad (20)$$

These branching reactions can greatly accelerate the oxidation (autocatalysis) and complicate the reaction picture. Another complication is that the increased reaction rate may drive the system out of the kinetic region (i.e., into a region where oxygen diffusion becomes a limitation). Therefore, this must be taken into account in high-temperature oxidation.

EXPERIMENTAL METHODS

Reaction kinetics of liquid-phase oxidation processes must be studied in the kinetic region. That is, the reaction must not be oxygen diffusion limited. Most standard oxidation-corrosion tests developed in the past have been bulk tests. Air or oxygen is passed over a static fluid, bubbled through the fluid or over a constantly agitated fluid. An example of a macro-oxidation

cell is shown in figure 8. It is not within the scope of this paper to describe these macrotests, many of which are diffusion limited. Reference 26 discussed various types of these reactors. Other standard tests are also discussed in the literature (refs. 62 and 63).

Oxygen Diffusion

Oxygen transport into the liquid-phase involves three processes.
(1) Diffusion of oxygen in the gas phase to the liquid-gas interface,
(2) Dissolution of oxygen into the liquid at the gas-liquid interface,
(3) Diffusion of the dissolved oxygen into the liquid phase.
Process (1) is very rapid and not a limiting factor. Process (2) is related to the partial pressure of oxygen and Henry's law constant. Process (3) depends on the interfacial surface area, rate of agitation, and the oxygen concentration gradient. Basically, to determine if oxygen diffusion is a problem, the amount of fluid or oxygen can be varied and agitation rates can be changed. If the rate of oxidation is altered, then the reaction is not taking place in the kinetic region.

Kinetic Curves

The most common parameter measured in most oxidation studies is the absorption of oxygen. If this parameter is plotted as a function of time, four different kinetic curves are observed (ref. 25) (fig. 9). Figure 9(a) shows an autocatalytic effect sometimes observed with mineral oils of low aromatic content. Figure 9(b) is autoretarding and an example is highly aromatic mineral oils. Figure 9(c) is linear and is neither autocatalytic nor autoretarding (a polybutene is an example). And finally, figure 9(d) shows mixed behavior (example - n-hexyldecylbenzene).

Microtests

Because of diffusion problems, many investigators have designed new experiments involving small quantities of fluid. A number of thin film tests have been developed (refs. 64 to 66). One of the most successful is that developed by Klaus and his coworkers (refs. 30 and 67).

This test is illustrated in figure 10. Basically, a very small quantity of lubricant (40 to 100 µl) is injected onto the surface of a catalyst after the entire apparatus has been equilibrated at test temperature. A constant flow of air is maintained through the air entry tube. Volatile oxidation products can be trapped for analysis. At the conclusion, which could be a few minutes or a few hours, depending on test temperature, the apparatus is removed from the oven or bath and quenched to room temperature.

Then, the degraded lubricant remaining on the catalyst surface is dissolved in an appropriate solvent. This solution can then be analyzed by a variety of techniques, some of which will be highlighted later. From this analysis, a rate of oxidation can be determined.

This apparatus has a number of advantages. It is simple, requires little test sample, has good reproducibility, and test durations are not long. Surface area is also constant and does not vary during the test. An infinite variety of catalysts can be studied and each can be recycled. However, there are some drawbacks.

The thin film test is a batch process and is subject to evaporation as well as oxidation. This usually can be taken into account by running identical tests in nitrogen. However, some highly stable materials require higher temperatures for reasonable reaction rates to take place. Sometimes the original charge disappears well before test conclusion. Of course, this can be alleviated by running tests above atmospheric pressure as has been done by others (ref. 25).

Another problem caused by the thin films is rapid loss of additives from formulated fluids. Even with thin film tests, diffusion limitations can occur, especially at high temperatures, where local oxygen consumption is great. In addition, these tests are usually run to high conversion (up to 50 percent). At high conversion the chain branching reactions which take place can greatly complicate the reaction picture. Here many products are formed and chemical analysis and kinetic treatment of the data become difficult if not impossible. Nevertheless this technique has been successful in reproducing high-temperature oxidation degradation from bearing tests (ref. 56), and gas turbine engine tests (ref. 68), and it has contributed to the fundamental understanding of the degradation of esters and hydrocarbons (ref. 69).

Stirred Flow Reactor

The thin film test just described is an example of a batch process. A single charge of material is used. In a continuous process, a constant flow of material to be oxidized is fed to the reactor. It has been shown that the instantaneous reaction rate can be determined by balancing the rate of reaction with this flow (ref. 70). This essentially maintains steady-state conditions. The stirred flow reactor is an example (ref. 34).

The material to be oxidized is fed into the reactor of constant volume in which there is thorough agitation producing a homogeneous mixture. This mixture is then removed at the same flow rate as the input of oxidizable material. Eventually, steady-state conditions will prevail and all reactants, intermediates, and final products have constant concentrations. The rate of consumption or formation of any product, intermediate, or reactant can then be calculated from the following equation.

$$\frac{d(X)}{dt} = \frac{(X)_\tau - (X)_0}{\tau} \tag{31}$$

where $d(X)/dt$ is the rate of consumption of formation of substance X, $(X)_\tau$ is the concentration of X in the effluent at steady state at residence time τ, and $(X)_0$ the concentration of X in the entering fluid.

This equation is valid for any species, regardless of the complexity of the reaction. This is obviously a plus for kinetic studies. An empirical rate

law can then be determined by finding a relationship that describes the rate of formation of a species as a function of its concentration in the reactor.

An example of a stirred flow microreactor is shown in figure 11. It consists of two pyrex spheres A and B. The inside sphere (B) is perforated. The hydrocarbon (RH) enters at the top and is mixed with a stream of oxygen. This mixture passes through the perforated sphere into sphere A. Theoretically, ideal mixing of the reactants, oxygen, and products occurs. The outlet is on the upper right.

This technique also has some drawbacks. Since a continuous flow of reactants is necessary, a much greater quantity of test material is required than in the thin film test. In addition, reactant purity must be stringently controlled. Nor is it clear how a catalytic surface could be incorporated. Although soluble metal catalysts could be incorporated in the reactant.

This type of apparatus has been successfully used in kinetic and mechanistic studies of n-hexadecane (refs. 34 and 35) and pentaerythrityl tetraheptanoate (PETH) (ref. 36). In addition, the mechanisms of two common antioxidants, 4,4-dioctyldiphenyl amine and 4,5-methylenebis (2,6-di-tert-butylphenol) (ref. 71) have been studied.

Microoxidation Corrosion Apparatus

Another microapparatus for batch operations is shown in figure 12. It is a modified version of the type reported by Snyder and Dolle (ref. 46). It consists of a pyrex decomposition tube and rod assembly. Metal catalysts may be positioned on the rod assembly. In a typical experiment, fluid is introduced into the decomposition tube. The system is evacuated and backfilled with oxygen to a known pressure. The tube is then placed in a preheated furnace for the specified test time. At test conclusion, the system is cooled and connected to a vacuum system. The liquid nitrogen noncondensibles are collected quantitatively, measured, and analyzed by various chemical means. The liquid nitrogen condensibles as well as the fluid residue are also analyzed. The rate of degradation is calculated from the amount of liquid nitrogen condensibles and is usually reported as milligrams of condensible product per gram of original fluid per hour of test.

This type of device has been used in a variety of studies on linear (ref. 52) and branched fluorinated polyethers (ref. 53). A similar device (only using flowing oxygen) was used to study a branched fluorinated polyether and a perfluoropolyether triazine (ref. 49).

Again this apparatus suffers from the same disadvantages as other batch reactors. Conditions must be chosen so as to eliminate oxygen depletion or diffusion problems.

Electronic Gas Sensor

As previously mentioned, both thermal and oxidative processes are accompanied by the evolution of gaseous hydrocarbon products. Ravner and Wohltjen

(ref. 72) have taken advantage of this fact to develop a rather simple technique for monitoring the oxidative breakdown of lubricants. They used a solid state metal oxide semiconductor gas sensor originally developed to detect explosive conditions. The system is diagrammed in figure 13. Correlation of the detected gas evolution with classical indicators of lubricant oxidation (such as viscosity and acid number changes) is illustrated in figure 14.

ANALYTICAL TECHNIQUES

During, or at test conclusion, a chemical analysis of the resulting products is necessary. A variety of common chemical analytical techniques are used for these analyses. The following sections are not meant to be an exhaustive survey of these techniques. The intent is just to highlight a few of the more commonly used procedures.

High Pressure Liquid Chromatography (HPLC)

The development of HPLC has afforded a method for the separation of complex mixtures of organic compounds (such as a mixture of oxidized lubricant products) (ref. 73). This method separates materials due to an equilibrium distribution of the materials between a stationary phase and a mobile phase which percolates through the stationary phase. HPLC is not used as extensively as gas chromatography (GC). However, it does have the advantage that while only about 20 percent of organic material is volatile enough for normal GC analysis, a greater percentage can be solubilized for separation by HPLC. An example of this separation technique in the size exclusion mode is described in the following paragraph.

Size Exclusion Chromatography

Size exclusion chromatography (SEC) is the HPLC mode that separates components of a mixture according to molecular size. G-MIL-99 is a generic gas turbine engine lubricant developed at NASA for fundamental tribological studies. It is very similar to proprietary blends meeting the MIL-L-23699 specification (ref. 74). G-MIL-99 is a single component basestock (trimethyolpropane triheptanoate) (TMPTH). This formulation also contains an antiwear additive (2.5 percent tricresyl phosphate (TCP), two antioxidants, 1 percent dioctyldiphenylamine (DODPA) and 1 percent phenyl-α-napthylamine (PANA), and a corrosion inhibitor, 0.02 percent benzotriazole (BTZ). Figure 15(a) is a SEC trace of the unused fluid using an ultraviolet detector at 254 nm. As can be seen, three of the four additives have been partially separated and are identified. Figure 15(b) contains the same sample but using a refractive index (RI) detector. Here, in addition to the additives, the primary ester peak is seen.

The next series of spectra (fig. 16) shows the progressive oxidation of a similar formulated ester in a gas turbine engine test (ref. 68). The spectra show the progressive loss of additives and the formation of higher molecular weight products. This data is typical of the decomposition seen in high-temperature tests with ester base fluids (refs. 29 and 69).

Ultraviolet-Visible Spectroscopy

Once an oxidized mixture has been separated, it is useful to chemically identify, at least qualitatively, the various components. Many lubricants and lubricant additives absorb light in the wavelength region of 200 to 800 nm. Aromatic compounds, in particular, adsorb strongly in the ultraviolet region (200 to 400 nm). These energy adsorptions are due to electronic transitions from ground to higher energy states. A diode-array spectrophotometer can be used to help identify various components as they elute from an HPLC column. This device is capable of measuring an entire ultraviolet-visible spectrum (UV-VIS) in 1 second. A series of UV-VIS spectra from the HMW region of figure 16 (65 hr sample) are shown in figure 17.

Infrared Spectroscopy

Another common identification technique is infrared spectroscopy (IR). Here the spectral region of interest is from 4800 to 400 cm^{-1}. Adsorptions in this region are due to various molecular vibrations such as stretching and bending motions. IR spectra for two components from a size exclusion chromatogram of an oxidized ester appear in figure 18. These spectra identify the undegraded ester basestock as well as the anti-wear additive (TCP).

Nuclear Magnetic Resonance

A third complimentary spectral technique is nuclear magnetic resonance (NMR). This technique may provide more structural information than either the IR or UV techniques. While IR and UV techniques are often empirical in nature, NMR requies a more theoretical basis for proper interpretation. Simply stated, many atomic nuclei possess magnetic moments. Normally, individual nuclear moments are randomly oriented so that there is no net magnetic moment. However, if that substance is placed between the poles of a powerful magnet, there will be a small net orientation with the external field. One can then measure the energy required to promote nuclei to high energy states, out of alignment with the field. An example of the use of NMR in oxidation studies is illustrated in figure 19.

Here a proton NMR spectrum of an as-received fluorinated polyether is shown in figure 19(a). The presence of a doublet in the NMR spectrum at 5.9 ppm is indicative of the presence of a C-H bond. This is confirmed by the spectrum of a fully characterized fluid ($C_3F_7OCF(CF_3)H$) known to contain a C-H bond (fig. 19(b)). The fluorinated polyether is supposed to be devoid of such bonds. Since the bond energy of a C-H bond is much less than that of a corresponding C-F bond, this presence of C-H in such a fluid provides an unwanted weak link. The consequences of this are discussed in the section on fluorinated polyethers. A spectrum of the same fluid after thermal pretreatment in oxygen at 343° C appears in figure 19(c). Here the C-H impurities have been degraded and the doublet has disappeared and a much more stable fluid results.

Electron Paramagnetic Resonance

Somewhat analogous to NMR is a technique known as electron paramagnetic resonance (EPR) (ref. 75). Here we are concerned with electrons rather than nuclei. The spin in a magnetic field may be oriented in two ways and each have slightly different energies. If radiation is supplied, a transition may occur. Radiation in the microwave region is used. In practice, the wavelength of the radiation is kept constant while the intensity of the magnetic field is varied. This method can detect unpaired electrons (free radicals) in concentrations as low as 10^{-7} molar (ref. 76).

An example of a stable (long-lived) free radical electrochemically generated C-ether lubricant is shown in figure 20. Actually, two free radicals are present. These species may be reaction products of initially generated radical ions and may be responsible for the rapid production of high molecular weight material (sludge) often generated by C-ethers in high-temperature bearing tests (refs. 54 and 56).

OTHER EXPERIMENTAL TECHNIQUES

Chemiluminescence

Chemiluminescence (CL) is simply light emitted from a chemical reaction. It was first observed in biological sources such as the firefly (ref. 77). If a reaction is to produce light several criteria must be met: (1) sufficient energy for excitation, (2) a species capable of forming an excited state, (3) an emitter to give off excitation energy, (4) a rapid chemical reaction, and (5) a reaction-coordinate system favoring production of an excited state over direct ground state formation.

It has been observed for many years that CL is associated with many oxidation processes (ref. 78). Referring back to the sequence of reactions in the autoxidation of hydrocarbons, it is believed that equation (13) is responsible for the observed CL:

$$2RO_2\cdot \rightarrow ROH + R_2C=O + O_2 \qquad (13)$$

$$\searrow (R_2C=O)^*$$

This disproportionation reaction produces a small amount of excited states $(R_2C=O)^*$. For most hydrocarbons, only one photon is emitted for each 10^8 to 10^{10} termination reaction. This inefficiency is caused, in part, by quenching reactions between the excited ketone with oxygen and other species.

$$(R_2C=O)^* + Q \rightarrow R_2C=O + Q \qquad (32)$$

$$(R_2C=O)^* \rightarrow R_2C=O + h\nu \qquad (33)$$

The intensity of the emitted radiation (hν) is directly proportional to the square of the concentration of peroxy radicals $[RO_2\cdot]^2$. This dependence is the basis for determining the concentration of peroxy radicals and thus the kinetics of hydrocarbon oxidation. The advantages of CL are (1) it is extremely sensitive, (2) it is noninvasive, (3) it provides a continuous monitor of peroxy radicals, and (4) only small samples are required. A number of investigators have used CL in oxidation studies (refs. 79 to 81). An example of a CL apparatus appears in figure 21. A thorough review of CL appears in reference 82 and a recent review concerning its applications to fuels and lubricants appears in reference 83.

Shock Tube Studies

Another method that has been used for kinetic studies of hydrocarbon pyrolysis and oxidation is the shock tube technique (ref. 84). Its use in gas phase hydrocarbon oxidation is reported in reference 85. In this technique, gas samples are heated during a very short time interval (0.5 to 5 μsec) and then quenched by expansion. The reaction products can then by analyzed outside the shock tube for use in kinetic studies. Since this analysis can be carried out at leisure, a variety of analytical methods can be used. Therefore, each experiment can yield data on the concentrations of many compounds. A variety of rate constants for various hydrocarbon reactions appear in reference 85.

CLASSES OF LUBRICANTS

Hydrocarbons

Most conventional automotive lubricants are mineral oils which are complex mixtures of hydrocarbons. Although some fundamental studies (refs. 20, 33, and 69) have examined these materials, others (refs. 34, 35, 38, 43, 44, 45, and 86) have opted to study a pure component.

Jensen and coworkers (refs. 34 and 35) have performed a series of elegant experiments with pure n-hexadecane. Autoxidation with molecular oxygen was carried out at 120° to 180° C using a stirred flow reactor. Initial studies concentrated on identifying the primary oxidation products at 120°, 160°, and 180° C. These primary products included mono-, di-, and trihydroperoxides, hydroperoxyketones, cyclic peroxides, and some trifunctional products. Negligible amounts of esters or acids were formed in these low conversion studies.

The hydroperoxides are formed by both interhydrogen and intrahydrogen abstraction reactions. Furthermore, it appeared that a high percentage of hydrogen abstractions were taking place by hydroxy radicals (•OH). It was felt that the intramolecular abstractions should play a role in the autoxidation of all n-alkanes larger than n-butane.

In a continuation of this work (ref. 35), secondary or cleavage products of the autoxidation of n-hexadecane were determined. Products at low conversion (2 percent or less) included methylketones, alkanoic acids, hydrogen per-

oxide, aldehydes, ethers, carbon dioxide, and carbon monoxide. At higher conversions (<16 percent) esters and γ-lactones are formed.

The basic mechanism proposed by the authors to account for the observed products is summarized as follows:

Chain initiation occurs via homolysis of hydroperoxides forming alkoxy (RO•) and hydroxy (•OH) radicals which subsequently abstract protons producing alkyl radicals (R•). The alkyl radicals (R•) react with oxygen producing peroxy radicals (RO_2•) which, in turn, abstract hydrogens intra- or intermolecularly producing mono-, di-, and trihydroperoxides. Chain termination occurs via bimolecular reactions of chain carrying peroxy radicals (RO_2•). Methyl ketones (CH_3COR) and alkanoic acids (RCO_2H) are formed by cleavage reactions of α,γ-hydroperoxy ketones (HOOR=O). Excess acid and other cleavage products are derived from reactions of alkoxyl radicals (RO•).

Esters

Most esters in use today as lubricants are gas turbine engine lubricants. Present formulations meeting military specifications MIL-L-23699 or MIL-L-7808 are either based on trimethyolpropane or pentrerythritol. These alcohols, which contain no β-hydrogens, are estrified with various acids to produce the final ester products. In practice these lubricants contain a mixture of compounds.

However, as in the case of hydrocarbons, utilizing a pure compound for oxidation studies is advantageous. Hamilton et al. (ref. 36) have studied the mechanism of the autoxidation of pentaerythrityl tetraheptanoate at 180° to 220° C. This was an analogous study to their work with n-hexadecane previously discussed.

The proposed reaction scheme for PETH is very similar to that reported for n-hexadecane and is reproduced in figure 22. Again it consists of initiation by hydroperoxide decomposition forming reactive free radicals (1), formation of monohydroperoxides by intermolecular hydrogen abstraction (3), and dihydroperoxides and hydroperoxyketones by intramolecular abstractions (4 and 4*). Chain termination proceeds via peroxy radical recombination (6). Secondary products of acids and methylketones are formed from hydroxyketones (7). In addition, high MW carboxy and acetyl substituted tetraesters will be formed.

A kinetic analysis comparing rate constants for the two systems (PETH and n-C_{16}) showed a remarkable similarity for most reaction steps. This would indicate that indeed both compounds appear to be reacting by a similar mechanism.

Continuing research at Pennsylvania State University over the last few years has also led to a fundamental understanding of the thermal-oxidative reactions taking place in ester based systems (refs. 27 to 32).

Bulk oxidation tests to (500° F) 260° C on di-2-ethylhexyl sebacate (DES) and trimethyolpropane triheptanoate (TMPTH) were reported by Czarnecki (ref. 28). At 260° C, tests with these esters were autoretarding (see fig. 9). It was felt that this was due to the in situ formation of inhibiting materials.

However, there were obvious oxygen diffusion limitations since an approximate 30 C° rise in test temperature only doubled the reaction rate.

Reaction products for both tests were analyzed by gas chromatography and mass spectroscopy. For DES a half acid ester and a high boiling fraction (>510° C) were reported.

For TMPTH, a diester and smaller fragments were reported as well as a high boiling fraction. No definitive reaction scheme was theorized but some sort of a condensation reaction was proposed for the formation of the high boiling (i.e., high molecular weight) fractions.

Ali (ref. 87) reported further on the chemical degradation of esters again using a bulk oxidation technique. Some diesters, TMPTH and PETH were studied. Oxidized products were separated by gel permeation chromatography. A chromatogram for di-2-ethylhexyl sebacate is shown in figure 23. Typically all the esters produced three fractions of low, intermediate, and high MW. The individual fractions were isolated and further analyzed by IR, UV, and NMR techniques. It was deduced that, initially, a low molecular weight product is formed which eventually polymerizes to a high MW sludge (fraction 3). Spectroscopic analysis indicated that the polymerized fraction (up to MW of 50 000) contained carbonyl groups conjugated with one or more double bonds (-C=C-C=O).

Cvitkovic (ref. 30) described the development of the microoxidation test previously discussed. Ester oxidation was represented by a simple phenomenological model. It was concluded that this technique adequately simulates severe degradation environments such as those present in high-temperature gas turbine engines.

Product analysis reinforced the theory that the first step in ester oxidation is the formation of low MW unstable species which subsequently polymerize into high MW sludge. UV absorption was found to increase with increasing MW of oxidation products and with the extent of oxidation. In addition GPC analysis combined with atomic absorption (AA) of samples from 4-ball tests indicate that the iron surface participates in the reactions generating high MW material.

Further work was reported by Lockwood et al. (refs. 32 and 88), with esters using the same apparatus. Here a kinetic model was devised which predicted inhibitor oxidation rates, evaporation rates, and lubricant stable life from 174° to 247° C. Post stable life tests with Fe catalysts indicated rapid basestock oxidation with the production of high MW products and organic iron products.

A model for ester oxidation is presented in reference 88. It is similar to that proposed by Hamilton et al (ref. 36) except that the model is carried further to indicate how a final condensation polymer containing carbonyl groups conjugated with double bonds could be formed by dehydration of β-hydroxy ketones.

$$R\text{-}CHCH_2CR \xrightarrow{-H_2O} RCH{=}CHC\text{-}R \qquad (34)$$

In addition a mechanism whereby an intermediate product of ketone condensation could react with an iron surface to produce soluble iron products was presented.

$$FeOH + R\text{-}CH\,CH_2CR \longrightarrow \longrightarrow \qquad (35)$$

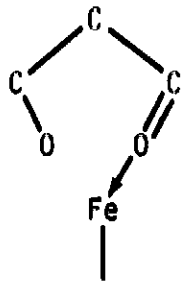

Polymeric product

Soluble iron products were almost totally suppressed by the presence of a known metal coater - TCP.

A further description of the Penn State microoxidation test appears in reference 69. Here oxidation tests of esters and a superrefined mineral oil are reported. Oxygen diffusion limitations were negligible for small samples (40 µl or less) at 245° C or less. Reaction kinetics indicated that esters and the mineral oil followed a first-order reaction rate from 0 time up to 80 percent conversion.

As indicated in previous work, primary oxidation products for the ester were of lower MW than was the basestock. For a mineral oil, these products were in the same MW region as the basestock. Secondary and tertiary reactions involve the primary reaction products in a condensation polymerization. The primary products do not accumulate. Therefore, it was concluded that primary oxidation is the rate determining step and the polymerization reaction is much more rapid.

Catalyst Studies

Catalyst studies indicated that the type of metal affects both the primary rate as well as the condensation step. For the primary reaction the following order of decreasing catalysis was observed:

Fe > Al > Pb > Cu

The order for decreasing catalysis of the condensation reaction was a little different:

Fe > Al > Cu > Pb

Qualitative analysis indicated that four characteristic chemical groups were identified in all oxidation products (primary and secondary) from esters and the mineral oil. These were hydroxyl (-OH), carbonyl (C=O), alkenes (C=C), and conjugated dienes (C=C-C=O).

More recent work (ref. 22) with the microreactor indicates that oxygen is definitely required to induce the polymerization reaction with esters. This work also established that while low carbon steel and stainless steel catalyze oxidation, Pb, Zn, Sn, and Cu act as inhibitors. AA analysis indicates that the concentration of dissolved metal in a lubricant does not follow the order of catalytic activity. Low concentrations of iron are active promoters while high concentrations of lead act as inhibitors.

Polyphenyl Ethers

The polyphenyl ether fluids have been studied (refs. 89 and 90) as possible high-temperature lubricants for many years. They are thermally stable to approximately 450° C and oxidatively stable to approximately 275° C. Most of their problems have been related to poor low-temperature properties and poor boundary lubricating ability.

Most of the mechanisms of oxidation degradation of these fluids were performed in the early 60's (refs. 55 and 91). At 288° C and above these fluids begin to consume oxygen (after an induction period). These were bulk oxidation tests using a Dornte type apparatus. As oxidation proceeds, the fluid turns black with an accompanying linear increase in viscosity with increasing oxygen consumption. In addition, EPR spectra indicated the presence of a stable free radical in the oxidized product.

In contrast to the previously discussed autoxidation mechanisms of aliphatic hydrocarbons, the initiation step appears to be an attack by molecular oxygen at the phenyl-oxygen-phenyl carbons rather than C-H positions. Symmetrical and unsymmetrical cleavage and dehydrogenation reactions occur to yield phenoxy and substituted phenoxy radicals.

Propagation occurs when these radicals attack the parent molecule at the C-O-C carbons producing more phenoxy radicals and with cleavage to form a higher molecular weight product (containing some C-C bridges). An overall reaction would be

$$5C_{24}H_{18}O_3 + 4O_2 \rightarrow 2OC_6H_4O_9 + 5H_2O \qquad (36)$$

Because of the inherent stability of these fluids, conventional antioxidants (such as amines and phenols) are not useful. This is related to the volatility or thermal instability of these additives. However, some additives are effective above 260° C. These include aromatic tin compounds such as tetraphenyl tin (ref. 92) and certain other organometallic compounds (ref. 91). Cuprous and cupric oxides (refs. 92 and 93) were also effective.

A continuation of this work (ref. 95) showed that soluble alkali or alkaline earth metal phenoxides are also effective inhibitors to 370° C. Oxides, hydroxides, and carbonates of alkali metals and barium are very effective in-

nibitors (to approximately 370° C). A proposed mechanism is the destruction of peroxy radicals by a superoxide formation (ref. 94).

In fact, oxidation/corrosion tests (ref. 96) showed that the presence of a variety of metal coupons reduced the oxidation of a polyphenyl ether (measured by viscosity increase). Lead and copper seemed to be the most effective. This is in agreement with the findings of Klaus et al. (ref. 22) discussed in the ester section.

C-Ethers

Another class of fluids, (C-ethers) or thio-ethers, are structurally similar to the polyphenyl ethers (ref. 97). The basic composition of this class is shown in figure 24. These fluids have certain advantages over the polyphenyl ethers such as lower pour points and better boundary lubricating performance (ref. 98). However, their inherent thermal stability is somewhat lower (approximately 390° C) and oxidation stability (bulk tests) is about 260° C. However, as with the polyphenyl ethers, these fluids do produce large quantities of a high molecular weight sludge under lubricating conditions (ref. 99).

Macro oxidation-corrosion tests of formulated C-ethers indicated deposit formation was a problem (ref. 54). Two C-ether formulations were studied by Jones and Morales (ref. 56) at 353° C using the Penn State a macro-reactor design. Degradation products were analyzed by gel permeation chromatography. M-50 steel and Ag were used as catalysts.

In general, both catalyzed C-ether decomposition to about the same extent. This is in contrast to the data reported in reference 54, where silver produced 2 to 5 times the amount of high molecular weight products as M-50 under similar test conditions. In addition there was little difference between air and nitrogen atmosphere tests based on high MW product formation.

Several discrete peaks of higher MW were seen on many of the chromatograms. Peaks appeared at about 450, 600, 700, and 800 as well as a broad peak centered at 2400 (see fig. 25). It would appear that coupling reactions resulting in a series of higher MW oligomers basically differing in MW by the addition of another phenyl-sulfur species. A process similar to that described for the polyphenyl ethers could be operating here.

Perfluoroalkylethers

Perfluoroalkylethers are a class of fluids which exhibits excellent thermal and oxidative stability (refs. 100 and 101). Combined with good viscosity characteristics (ref. 43), good elastohydrodynamic film forming capabilities (ref. 102), good boundary lubricating ability (refs. 46 and 49), and nonflammability properties (ref. 51) make these fluids promising candidates for high-temperature lubricant applications.

Basically, there are two types of perfluoroalkylethers, an unbranched and a branched class. The general structures of these classes are shown in figure 26. The most important representatives of the branched materials (fig. 26(a)) are based on the polymerization of hexafluoropropylene oxide (HFPO).

Branched Perfluoroalkylethers

Initial thermal and oxidative stability tests on the branched class were performed on very pure, highly characterized materials (ref. 100). This early data indicated that these materials should be thermally stable to 410° C and that oxygen would not accelerate this degradation.

However, tests performed on commercial samples never yielded this idealized stability. Thermal stability of about 390° C (ref. 49) and oxidation/corrosion stability to 260° C (ref. 46) in the presence of ferrous and titanium alloys was obtained. This was confirmed by Paciorek et al. (ref. 47) in bulk oxidation/corrosion experiments.

In the early work by Gumprecht (ref. 103) he showed that pure (i.e., completely fluorinated) HFPO fluids theoretically yield mainly $CF_3CF{=}CF_2$, CF_3COF, and COF_2. Under oxidizing conditions (Paciorek et al.) (ref. 47) did not observe any $CF_3CF{=}CF_2$. This may be due to the oxidation reaction

$$CF_3CF{=}CF_2 \rightarrow CF_3\overset{O}{\overset{\|}{C}}F + COF_2 \qquad (37)$$

or more likely due to the unzipping reaction

$$\sim\!\!\sim\!\!\text{CF}(\text{CF}_3)\text{-CF}_2\text{O}\ \text{CF}(\text{CF}_3)\text{-CF}_2\text{O}\cdot \rightarrow CF_3\overset{O}{\overset{\|}{C}}F + COF_2 \qquad (38)$$

The major products isolated at test conclusion were SiF_4, CO_2, and BF_3. These are obviously due to reaction of the primary products with the glass surface of the oxidation-corrosion apparatus such as

$$2COF_2 + SiO_2 \rightarrow SiF_4 + 2CO_2 \qquad (39)$$

Based on the rate of production of these volatile products, it was determined that the commercial HFPO fluids were oxidatively stable to about 343° C in the absence of metal. The limited degradation at 343° C was thought to be due to oxidative instability of a weak link or end group. Since at test conclusion the residual fluid was essentially unchanged (i.e., same MW, viscosity, and IR spectra), it was deduced that a certain number of chains had to be hydrogen terminated. Indeed, pretreatment at 343° C with oxygen yielded a more stable fluid, presumably due to burning off the weak hydrogen terminated chains. Proton NMR (fig. 19) eventually confirmed this theory. The as-received fluid shows the presence of CF_3CFHO - as a characteristic doublet at 5.9 ppm. After thermal-oxidative exposure at 343° C these peaks completely disappear (fig. 19(c)).

In the presence of metals and alloys at 316° C such as Ti (4 Al, 4 Mn), Ti, and Al, the degradation rate is increased (fig. 27) and is higher for the nonpretreated fluid. This would indicate that the metals are accelerating the

degradation of weak links. However, successive measurements with the Ti (4 Al, 4 Mn) alloy at 288° C show a continual uptake of oxygen with time. Obviously another mechanism is operative here. Analysis of the residual fluid showed a drastic decrease in MW which would indicate that a chain scission process is likely, such as depicted below

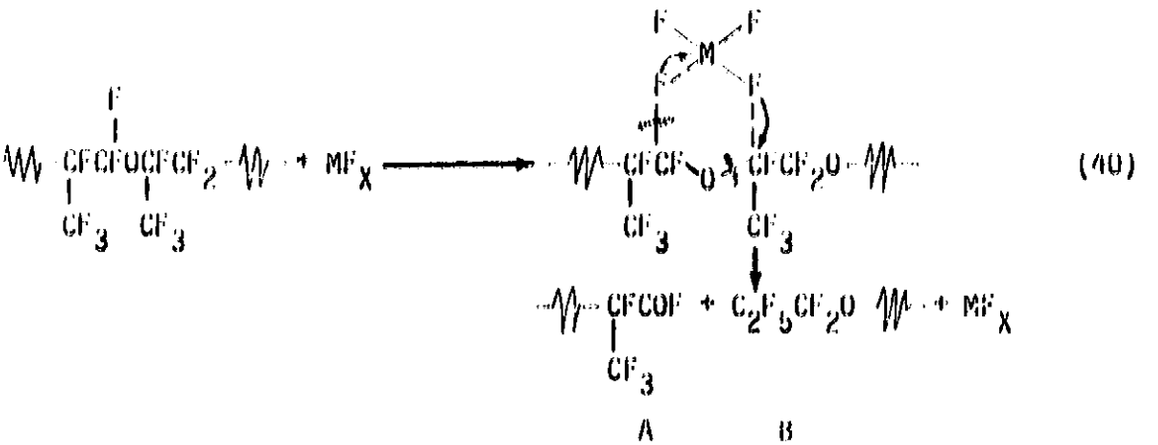

(40)

Fragment A can further degrade and B is just a lower MW telomer of the HFPO fluid.

Therefore, it appears that metals and metal alloys promote degradation in HFPO fluids by a chain scission process. The HFPO fluids that have been thermally pretreated at 343° C in oxygen are stable to oxygen at this temperature. Nor is the pretreated fluid degraded by M-50 steel or Ti (4 Al, 4 Mn) alloys at 316° C. However, degradation does occur at 343° C with these alloys.

Unbranched Perfluoroalkylethers

A new class of perfluoroalkylethers based on the photo-oxidation of fluoro-olefins (ref. 104) has been developed. This class of materials, whose general chemical structure appears in figure 26(b), has an unbranched structure (no pendant CF_3 groups). These fluids have better viscosity-temperature properties than the branched (HFPO) class (ref. 50). However, the linear fluid class has exhibited lower thermal-oxidative stability compared to the HFPO fluids (ref. 50). This is surprising since the chemical bonding in both classes is very similar. In fact, it has been shown (ref. 103) that tertiary carbon-fluorine bonds are less stable than those involving primary or secondary carbon atoms. This would lead one to conclude that the HFPO fluids (which contain tertiary carbon atoms) should be less stable than the linear fluids.

Recent work (ref. 52) has confirmed that the unbranched fluids are inherently unstable at 316° C in oxidizing atmospheres. This instability is not due to hydrogen chain termination or residual peroxide linkages. In the presence of M-50 steel or Ti (4 Al, 4 Mn) alloys at 288° and 316° C in oxidizing atmospheres, the unbranched fluids exhibit much greater degradation than in uncatalyzed tests (fig. 28). However, these alloys do not promote degradation at 316° C in inert (nitrogen) atmospheres.

In addition, catalyzed tests indicated that pure metals (Ti, Al) did not promote as much degradation as alloys [Ti (4 Al, 4 Mn)] (fig. 29). Again, as

with the HFPO fluids, the metals and alloys promoted degradation via a chain scission process which is depicted in figure 30.

Inhibitors

Two different degaradation inhibitors have been studied with perfluoroalkylether fluids, a perfluorophenyl phosphine (P-3) (refs. 48 and 52) and a phosphatriazine (C_2PN_3) (ref. 52). Both of these inhibitors have been shown to be quite effective at 298° C in oxygen with the unbranched fluids (fig. 31), but are only marginally effective at 316° C. Similar responses occurred with the branched fluids (ref. 53).

MODELING AND SIMULATION

In the last 10 years, modeling (ref. 105) has been increasingly used in the study of complex reactions (ref. 106), including oxidation (ref. 107). Modeling involves a systemization of information for a particular complex reaction. This systemization should lead to a compilation of all possible mechanisms. This results in a chaotic set of chemical reactions.

Next this set of reactions is systematized into a network. In particular, to a sequence network which will describe the possible pathways of given atoms via certain selected species. An example of a sequence network for the oxidation of ethylbenzene (RH_2) is shown in figure 32. Experimental data then provides feedback for the initial mechanism compilation. Reactions found not to occur may be eliminated while others may be added. Certain experiments (in vitro) may be performed for additional information. For example, the importance of a specific subset of reactions may be studied by excluding other competing reactions.

It is obviously important to determine the relationship between the reaction mechanism and kinetics. Any mechanism can be expresssed by the following differential equation system

$$\underline{C} = \underline{A} \cdot (\underline{k} \cdot \underline{c}) \tag{41}$$

where $\underline{C}$ is the column vector of the first derivative of the species concentrations with time, $\underline{A}$ is the stoichiometric matrix determined by the mechanism, $\underline{k}$ is the rate constant matrix of the elementary processes in the mechanism, and $\underline{c}$ is the column vector of the time dependence of the species concentration.

There are three analysis possibilities:

(1) Only the important reactions are considered (zeros are inserted in the $\underline{A}$ matrix for eliminated reactions) and the reduced system solved.

(2) The concentrations of all species are measured and the equations solved for $\underline{k}$.

(3) By arbitrarily varying the elements of $\underline{k}$, different solutions may be obtained and then compared with experimental data. This enables one to determine the importance of the various reactions in the overall mechanism. This approach is called computer simulation.

A detailed explanation for a modeling process for the liquid phase oxidation of ethylbenzene appears in reference 107. A general introduction to simulation appears in reference 108.

GLOSSARY

Free Radical	A species having an unpaired electron but no charge
Homolysis	Breaking of a diamagnetic molecule into two paramagnetic species
Autoxidation	Oxidation of an organic compound with molecular oxygen in the absence of a flame
Catalyst	Any substance that increases the rate of a chemical reaction
Initiator	A substance that starts a free radical chain process
Oxidation	Electron removal from a chemical species
Disproportionation	Transfer of an atom from one radical to another forming a saturated and an unsaturated molecule
Lewis Acid	Species capable of accepting an electron pair

SYMBOLS

A	preexponential factor
AA	atomic absorption spectroscopy
Aro•	phenoxyl radical
CL	chemiluminescence
DES	di-2-ethylhexyl sebacate
E	activation energy
E_{DIS}	bond dissociation energy
ESR	electron spin resonance spectroscopy
HO_2•	hydroperoxy radical
In	initiator
IR	Infrared spectroscopy
k	rate constant
k_p	rate of chain propagation
k_t	rate of chain termination
MW	molecular weight
NMR	nuclear magnetic resonance spectroscopy
PETH	pentaerythrityl tetraheptanoate

PTZ	phenothiazine
R	gas constant
R-H	hydrocarbon
R•	rate of chain initiation
RO•	alkyl free radical
RO_2•	alkoxy radical
RO_2I	peroxy radical
RO_2H	hydroperoxide
RO_4R	tetroxide
SEC	size exclusion chromatography
T	absolute temperature
T_D	thermal decomposition temperature
TCP	tricresyl phosphate
TMPTH	trimethyolpropane triheptanoate
UV	ultraviolet spectroscopy
X	inhibitor

REFERENCES

1. Bisson, E. E.; and Anderson, W. J.: Advanced Bearing Technology. NASA SP-38, 1964.

2. Loomis, W. R.; Townsend, D. P.; and Johnson, R. L.: Lubricants for Inerted Lubrication Systems in Engines for Advanced Aircraft. NASA TN D-5420, Sept. 1969.

3. Parker, R. J.; Bamberger, E. N.; and Zaretsky, E. V.: Bearing Torque and Fatigue Life Studies with Several Lubricants for Use in the Range 500° to 700° F. NASA TN D-3948, May 1967.

4. Zaretsky, E. V.; and Ludwig, L. P.: Advancements in Bearings, Seals, and Lubricants. Aircraft Propulsion, NASA SP-259, 1971, pp. 421-463.

5. Sliney, H. E.: Bearings, Lubricants, and Seals for the Space Shuttle. Space Transportation System Technology Symposium, Vol. III - Structures and Materials, NASA TM X-52876, 1970, pp. 289-296.

6. Bucknell, R. L.: Influence of Fuels and Lubricants on Turbine Engine Design and Performance, Vol. II - Fuel and Lubricant Analyses. PWA-FR-5673, AFAPL-TR-73-52-VOL-2, Pratt and Whitney Aircraft, 1973. (AD-769309.)

7. Lansdown, A. R.: Liquid Lubricants - Functions and Requirements. Interdisciplinary Approach to Liquid Lubricant Technology, P. M. Ku, ed., NASA SP-318, 1973, pp. 1-55.

8. Russell, T. E.; and Mattes, R. E.: A Study of High Temperature Fuels and Lubricants on Supersonic Aircraft/Engine System Performance. SAE Paper 740473, Apr. 1974.

9. Kochi, J. K., ed.: Free Radicals. Vol. I, Wiley, 1973.

10. Back, M. H.: Pyrolysis of Hydrocarbons. The Mechanisms of Pyrolysis, Oxidation, and Burning of Organic Materials, L. A. Wall, ed., NBS SP-357, 1972, pp. 17-31.

11. Layokun, S. K.; and Slater, D. H.: Mechanism and Kinetics of Propane Pyrolysis. Ind. Eng. Chem. Process. Des. Dev., vol. 18, no. 2, 1979, pp. 232-236.

12. Blake, Edward S.; et al.: Thermal Stability as a Function of Chemical Structure. J. Chem. Eng. Data, vol. 6, no. 1, Jan. 1961, pp. 87-98.

13. Vapor Pressure-Temperature Relationship and Initial Decomposition Temperature of Liquids by Isoteniscope. Am. Soc. Test. Mater. Stand. D-2879-75, Part No. 24, 1980.

14. Fowler, L.; and Trump, W. N.: A Recording Tensimeter and Decomposition Temperature Detector. Analysis Instrumentation, Vol. 7. B. Connelly, L. Fowler, and R. Krueger, eds., ISA, 1969, pp. 141-144.

15. Jones, W. R., Jr.; and Hady, W. F.: Boundary Lubrication and Thermal Stability Studies with Five Liquid Lubricants in Nitrogen to 400° C. NASA TN D-6251, Mar. 1971.

16. Beerbower, A.: Environmental Capability of Liquid Lubricants. Interdisciplinary Approach to Liquid Lubricant Technology, P. M. Ku, ed., NASA SP-318, 1973, pp. 365-431.

17. Jones, W. R., Jr.: Friction, Wear, and Thermal Stability Studies of Some Organotin and Organosilicon Compounds. NASA TN D-7175, Mar. 1973.

18. Richardson, G. A.; and Blake, E. S.: Partially Fluorinated Polyaromatic Ethers: Synthesis, Thermal Stability, and Other Physical Properties. USAF Aerospace Fluids and Lubricants Conf., P. M. Ku, ed., Southwest Research Inst., 1963, pp. 130-139.

19. Gunderson, R. C.; and Hart, A. W.: Synthetic Lubricants. Reinhold Publ. Corp., 1962.

20. Klaus, E. E.; and Perez, J. M.: Thermal Stability Characteristics of Some Mineral Oil and Hydrocarbon Hydraulic Fluids and Lubricants. ASLE Trans., vol. 10, 1967, pp. 38-47.

21. Van Krevelen, D. W.: Properties of Polymers, Their Estimation and Correlation with Chemical Structure. Second ed., Elsevier Scientific Publ. Co. (Amsterdam), 1976.

22. Ugwuzor, D.I.K.A.: The Effects of Metals on High Temperature Degradation of Ester-Type Lubricants. M.S. Thesis, Penn. State Univ., Nov. 1982.

23. Backstrom, H.L.J.: The Chain-Reaction Theory of Negative Catalysis. J. Am. Chem. Soc., vol. 49, no. 6, June 1927, pp. 1460-1472.

24. Criegee, R.; Pilz, H.; and Flygare, H.: Olefin Peroxides. Chem. Ber., vol. 72B, 1939, pp. 1799-1804.

25. Emanuel, N. M.; Denisov, E. T.; and Maizus, Z. K. {(B. J. Hazzard, Transl.)}: Liquid Phase Oxidation of Hydrocarbons. Plenum, 1967.

26. Dukek, W. G.: Fuels and Lubricants for the Next Generation Aircraft - the Supersonic Transport. J. Inst. Pet. London, vol. 50, no. 491, 1964, pp. 273-296.

27. Booser, E. R.: Liquid-Phase Oxidation of Pure Hydrocarbons. Ph.D. Thesis, The Pennsylvania State University, 1968.

28. Czarnecki, J. R.: High Temperature Degradation of Some Organic Esters. M.S. Thesis, The Pennsylvania State University, Sept. 1971.

29. Ali, A. R.: Characterization of Liquid Phase Oxidation Products. M.S. Thesis, Pennsylvania State University, 1975.

30. Cvitkovic, E.: Reaction Rate Studies on Ester Oxidation. M.S. Thesis, Pennsylvania State University, May 1976.

31. Lahijani, J.: Effects of Metals on Oxidation Rates and Products from Esters. M.S. Thesis, Pennsylvania State University, 1977.

32. Lockwood, F. E.: Ester Oxidation Under Simulated Boundary Lubrication Conditions. Ph.D. Thesis, Pennsylvania State University, 1978.

33. Korcek, S.; and Jensen, R. K.: Relation Between Base Oil Composition and Oxidation Stability at Increased Temperatures. ASLE Trans., vol. 19, no. 2, 1976, pp. 83-94.

34. Jensen, R. K.; et al.: Liquid-Phase Autoxidation of Organic Compounds at Elevated Temperatures. 1. The Stirred Flow Reactor Technique and Analysis of Primary Products from n-Hexadecane Autoxidation at 120°-180° C. J. Am. Chem. Soc., vol. 101, no. 25, Dec. 1979, pp. 7574-7584.

35. Jensen, R. K.; et al.: Liquid-Phase Autoxidation of Ogranic Compounds at Elevated Temperatures. 2. Kinetics and Mechanism of the Formation of Clevage Products in n-Hexadecane Autoxidation. J. Am. Chem. Soc., vol. 103, no. 7, Apr. 1981, pp. 1742-1749.

36. Hamilton, E. J.; et al.: Kinetics and Mechanism of the Autoxidation of Pentaerythrityl Tetraheptanoate at 180-220° C. Int. J. Chem. Kinet., Vol. 12, no. 9, 1980, pp. 577-603.

37. Mahoney, L. R.; et al.: Effects of Structure on the Thermoxidative Stability of Synthetic Ester Lubricants: Theory and Predictive Method Development. Presented at the Div. of Petrol. Chem., Amer. Chem. Soc. (Las Vegas, Nev.), Mar. 28-Apr. 2, 1982.

38. Boss, B. D.; and Hazlett, R. N.: Oxidation of Hydrocarbons in the Liquid Phase - n-Dodecane in a Borosilicate Glass Chamber at 200° C. Can. J. Chem. vol. 47, 1969, pp. 4175-4182.

39. Mill, T.; et al.: Gasand Liquid-Phase Oxidation of n-Butane. J. Am. Chem. Soc., vol. 94, no. 19, Sept. 1972, pp. 6802-6811.

40. Van Sickle, D. E.; et al.: Intramolecular Propagation in the Oxidation of n-Alkanes, Autoxidation of n-Pentane and n-Octane. J. Org. Chem., vol. 38, no. 26, 1973, p. 4435.

41. Brown, D. M.; and Fish, A.: The Extension to Long-Chain Alkanes and to High Temperatures of the Hydroperoxide Chain Mechanism of Autoxidation. Proc. R. Soc. London Ser. A, vol. 308, no. 1495, Jan. 1969, pp. 547-568.

42. Snieyoski, P. J.: Selectivity of the Oxidative Attack on a Model Ester Lubricant. ASLE Trans., vol. 20, no. 4, 1977, pp. 282-286.

43. Betts, J.: Kinetics of Hydrocarbon Autoxidation in the Liquid Phase. Quart. Rev. Chem. Soc., vol. 25, no. 2, 1971, pp. 265-288.

44. George, P.; Rideal, E. K.; and Robertson, A.: Oxidation of Liquid Hydrocarbons. Proc. R. Soc. London, vol. 185, no. 1002, Mar. 1946, pp. 288-351.

45. Morton, F.; and Bell, R. T. T.: Low-Temperature, Liquid-Phase Oxidation of Hydrocarbons. J. Inst. Pet. London, vol. 44, 1958, pp. 260-272.

46. Snyder, C. E., Jr.; and Dolle, R. E., Jr.: Development of Polyperfluroalkylethers as High Temperature Lubricants and Hydraulic Fluids. ASLE Trans., vol. 19, 1976, pp. 171-180.

47. Paciorek, K. J. L.; et al.: Thermal Oxidative Studies of Poly (Hexafluoropropene Oxide) Fluids. J. Appl. Polym. Sci., vol. 24, no. 6, 1979, pp. 1397-1411.

48. Snyder, C. E. Jr.; et al.: Synthesis and Development of Improved High-Temperature Additives for Perfluoroalkylether Lubricants and Hydraulic Fluid. Lubr. Eng., vol. 35, no. 8, Aug. 1979, pp. 451-456.

49. Jones, W. R. Jr.; and Snyder, C. E., Jr.: Boundary Lubrication, Thermal and Oxidative Stability of a Fluorinated Polyether and a Perfluoropolyether Triazine. ASLE Trans., vol. 23, no. 3, July 1980, pp. 253-261.

50. Snyder, C. E. Jr.; Gschwender, L. J.; and Tamborski, C.: Linear Polyperfluoroalkylether - Based Wide-Liquid-Range High-Temperature Fluids and Lubricants. Lubr. Eng., vol. 37, no. 6, June 1981, pp. 344-349.

51. Snyder, C. E. Jr.; Gschwender, L. J.; and Cambell, W. B.: Development and Mechanical Evaluation of Nonflammable Aerospace (-54° C to 135° C) Hydraulic Fluids. Lubr. Eng., vol. 38, no. 1, Jan. 1982, pp. 41-51.

52. Jones, W. R. Jr.; et al.: Thermal Oxidative Degradation Reactions of Linear Perfluoroalkylethers. NASA TM-82834, Apr. 1982.

53. Jones, W. R. Jr.; et al.: Metals and Inhibitors Effects on Thermal Oxidative Degredation Reactions of Perfluoroalkylethers. Presented at the Sixth Winter Symposium on Fluorine Chemistry (Daytona Beach, Fla.), Feb. 6-11, 1983.

54. Clark, F. S.; and Miller, D. R.: Formulation and Evaluation of C-Ether Fluids as Lubricants Useful to 260° C. (MRC-SL-1007, Monsanto Research Corp.; NASA Contract NAS3-19746.) NASA CR-159794, Dec. 1980.

55. Wilson, G. R.; Smith, J. O.; and Stemniski, Jr.: Mechanism of Oxidation of Polyphenyl Ethers. ML TDR-64-98, Wright-Patterson AFB, Dec. 1963 (Available as AD-457120).

56. Jones, W. R. Jr.; and Morales, W.: Thermal and Oxidative Degradation Studies of Formulated C-Ethers by Gel-Permeation Chromatography. NASA TP-1994, Mar. 1982.

57. Sheldon, R. A.; and Kochi, J. K.: Metal-Catalyzed Oxidations of Organic Compounds. Academic Press, 1981.

58. Emanuel, N. M.: 80's in the Field of Liquid Phase Oxidation of Organic Compounds. Oxidation Communications, vol. 2, No. 3-4, 1982, pp. 221-238.

59. Korcek, S.; et al.: Absolute Rate Constants For Hydrocarbon Autoxidation XXI. Activation Energies for Propagation and the Correlation of Propagation Rate Constants with Carbon-Hydrogen Bond Strengths, Can. J. Chem., vol. 50, 1972, pp. 2285-2297.

60. Howard, J. A.: Absolute Rate Constants for Reactions of Oxyl Radicals. Advances in Free-Radical Chemistry, G. H. Williams, ed., Academic Press, 1972, pp. 49-165.

61. Bennett, J. E.; Brown, D. M.; and Mile, B.: Electron Spin Resonance of the Reactions of Alkylperoxy Radicals. I. Absolute Rate Constants for the Termination Reactions of Alkylperoxy Radicals. Trans. Faraday Soc., vol. 66, no. 2, 1970, pp. 386-396.

62. Dornte, R. W.: Oxidation of White Oils. Ind. Eng. Chem., vol. 28, Jan. 1936, pp. 26-30.

63. Bolland, J. L.: Kinetic Studies in the Chemistry of Rubber and Related Materials. I. The Thermal Oxidation of Ethyl Linoleate. Proc. R. Soc. London, vol. 186A, no. 1005, July 1946, pp. 218-236.

64. Diamond, H.; Kennedy, H. C.; Larsen, R. G.: Oxidation Characteristics of Lubricating Oils at High Temperature. Ind. Eng. Chem., vol. 44, 1952, pp. 1834-1843.

65. Brook, J. H. T.: A Circulatory (Oil) Oxidation Test. J. Inst. Pet. London, vol. 48, 1962, pp. 7-12.

66. Hepplewhite, H. L.; and Oberright, E. A.: Thin Film Oxidation Test of Lubricants for Gas Turbine Engines. Proc. USAF Aerospace Fluids and Lubricants Conf., P. M. Ku, ed., Southwest Research Inst., 1963, pp. 62-69.

67. Cvitkovic, E.; Klaus, E. E.; and Lockwood, F.: A Thin-Film Test For Measurement of the Oxidation and Evaporation of Ester-Type Lubricants. ASLE Trans., vol. 22, no. 4, 1979, pp. 395-401.

68. Jones, W. R. Jr.; and Morales, W.: Analysis of a MIL-L-27502 Lubricant From a Gas-Turbine Engine Test by Size-Exclusion Chromatography. NASA TP-2063, Jan. 1983.

69. Klaus, E. E.; et al.: Stability Studies of Organic Acid Ester Lubricants. Pennsylvania State Univ. Annual Rep. for NASA Grant NAG3-35, Mar. 1981.

70. Denbigh, K. G.: Velocity and Yield in Continuous-Reaction Systems. Trans. Faraday Soc., vol. 40, 1944, pp. 352-373.

71. Mahoney, L. R.; et al.: Time-Temperature Studies of High Temperature Deterioration Phenomena in Lubricant Systems: Synthetic Ester Lubricants. AFOSR TR-80-0065, Ford Motor Co., 1979. (AD-A080135.)

72. Ravner, H.; and Wohltjen, H.: The Determination of the Oxidative Stability of Several Deuterated Lubricants by an Electronic Gas Sensor. ASLE Preprint 82-AM-5A-4, May 1982.

73. Morales, W.: Use of High Pressure Liquid Chromatography in the Study of Liquid Lubricant Oxidation. NASA TM-83033, Oct. 1982.

74. Lubricating Oil, Aircraft Turbine Engine, Synthetic Base. MIL-L-23699C, Dept. of Defense, June 1981.

75. Assenheim, H. M.: Introduction to Electron Spin Resonance. Hilger and Watts, LTD (London), 1966.

76. Gould, E. S.: Inorganic Reactions and Structure. Halt, Rinehart, and Winston, Inc., 1962.

77. Harvey, E. N.: Bioluminescence, Academic Press, 1952.

78. Vassil'ev, R. F.: Chemiluminescence in Liquid-Phase Reactions. Progress in Reaction Kinetics, vol. 4, G. Porter, ed., Pergamon Press, 1967, pp. 305-352.

79. Slawinski, J.: The Use of Chemiluminescence for Investigation of the Kinetics of the Oxidation fo Hydrocarbons in the Liquid Phase. Int. Chem. Engr., vol. 6, no. 1, Jan. 1966, pp. 160-162.

80. Lloyd, R. A.: Low Level Chemiluminescence from Hydrocarbon Autoxidation Reactions. Part I. Apparatus for Studying Thermal Decomposition Reactions and Observations on Benzoyl Peroxide in De-oxygenated Benzene. Trans. Faraday Soc., vol. 61, no. 514, 1965, pp. 2173-2181.

81. Lloyd, R. A.: Thermal Decomposition of Benzoyl Peroxide, Cumene Hydroperoxide, and UV Irradiated Solvents. Part II. Low Level Chemiluminescence From Hydrocarbon Auto-oxidation Reactions. Trans. Faraday Soc., vol. 61, no. 514, 1965, pp. 2182-2193.

82. Hercules, D. M.: Physical Basis of Chemiluminescence. The Current Status of Liquid Scintillation Counting, E. D. Bransome, ed., Grune and Stratton, 1970, pp. 315-336.

83. Clark, D. B.; Weeks, S. J.; and Hsu, S. M.: Chemiluminescence of Fuels and Lubricants - A Critical Review. ASLE Preprint 82-AM-5A-1, May 1982.

84. Belford, R. L.; and Strehlow, R. A.: Shock Tube Technique in Chemical Kinetics. Ann. Rev. Phys. Chem., vol. 20, 1969, pp. 247-272.

85. Khandelwol, S. C.; and Skinner, G. B.: Shock Tube Studies of Hydrocarbon Oxidation Shock Waves in Chemistry. A. Liftshitz, ed., Marcel Dekker, 1981, pp. 1-57.

86. Larsen, R. G.; Thorpe, R. E.; and Armfield, F. A.: Oxidation Characteristics of Pure Hydrocarbons. Ind. Eng. Chem., vol. 34, no. 2, Feb. 1942, pp. 183-193.

87. Ali, A.; et al.: The Chemical Degradation of Ester Lubricants. ASLE Trans., vol. 22, no. 3, July 1979, pp. 267-276.

88. Lockwood, F.; and Klaus, E. E.: Ester Oxidation - The Effect of an Iron Surface. ASLE Trans., vol. 25, no. 2, 1982, pp. 236-244.

89. Mahoney, C. L.; et al.: Meta-Linked Polyphenyl Ethers as High-Temperature Radiation-Resistant Lubricants. ASLE Trans., vol. 3, no. 1, Apr. 1960, pp. 83-92.

90. Jones, W. R., Jr.; Hady, W. F.; and Swikert, M. A.: Lubrication With Some Polyphenyl Ethers and Superrefined Mineral Oils in a 600° F (316° C) Inerted Vane Pump Loop. NASA TN D-5096, Mar. 1969.

91. Archer, W. L.; and Bozer, K. B.: Oxidative Degradation of the Polyphenyl Ethers. Ind. Eng. Chem. Prod. Res. Develop., vol. 5, no. 2, June 1966, pp. 145-149.

92. Smith, J. O.; et al.: Research on High Temperature Additives for Lubricants. WADC-TR-59-191, Part IV, Feb. 1962. (Available as AD 281831.)

93. Ravner, H.; Russ, E. R.; and Timmons, C. O.: Antioxidant Action of Metals and Metal-Organic Salts on Fluoresters and Polyphenyl Ethers. J. Chem. Eng. Data, vol. 8, no. 4, Oct. 1963, pp. 591-596.

94. Ravner, H.; Moniz, W. B.; and Blachly, C. H.: High Temperture Stabilization of Polyphenyl Ethers by Inorganic Salts. ASLE Trans., vol. 15, no. 1, 1972, pp. 45-53.

95. Ravner, H.; and Kaufman, S.: High-Temperature Stabilization of Polyphenyl Ethers by Soluble Metal-Organic Salts. ASLE Trans., vol. 18, no. 1, 1975, pp. 1-4.

96. Stemniski, J. R.; et al.: Antioxidants for High-Temperature Lubricants. ASLE Trans., vol. 7, 1964, pp. 43-54.

97. McHugh, K. L.; and Stark, L. R.: Properties of a New Class of Polyaromatics for Use as High-Temperature Lubricants and Functional Fluids. ASLE Trans., vol. 9, no. 1, Jan. 1966, pp. 13-23.

98. Jones, W. R., Jr.: Boundary Lubrication of Formulated C-Ethers in Air to 300° C. Lubr. Eng., vol. 32, no. 10, 1976, pp. 530-538.

99. Jones, W. R., Jr.: The Effect of Oxygen Concentration on the Boundary-Lubricating Characteristics of a C-Ether and a Polyphenyl Ether to 300° C. Wear, vol. 73, 1981, pp. 123-136.

100. Gumprecht, W. H.: PR-143-A New Class of High Temperature Fluids. ASLE Trans., vol. 9, no. 1, Jan. 1966, pp. 24-30.

101. Sianesi, D.; et al.: Perfluoropolyethers - Their Physical Properties and Behavior at High and Low Temperatures. Wear, vol. 18, 1971, pp. 85-100.

102. Jones, W. R., Jr.; et al.: Pressure-Viscosity Measurements for Several Lubricants to 5.5×10^8 Newtons per Square Meter (8×10^4 psi) and 149° C (300° F). ASLE Trans., vol. 18, no. 4, 1975, pp. 249-262.

103. Gumprecht, W. H.: The Preparation and Thermal Behavior of Hexafluoropropylene Epoxide Polymers. Presented at the Fourth International Symposium on Fluorine Chemistry (Estes Park, Colorado), July 1967.

104. Sianesi, D.; et al.: Perfluoropolyethers by Photo-Oxidation of Fluoroolefins. Chim. Ind. (Milan), vol. 55, no 2, 1973, pp. 208-221.

105. Franks, R. G. E.: Modeling and Simulation and Chemical Engineering. John Wiley and Sons, Inc., 1972.

106. Happel, J.; and Sellers, P. H.: Multiple Reaction Mechanisms in Catalysis. Ind. Eng. Chem., Fundam., vol. 21, no. 1, 1982, pp. 67-76.

107. Gal, D.; et al.: Some Aspects of Modeling Hydrocarbon Oxidation. Eighteenth Symposium (International) on Combustion, The Combustion Institute, 1981, pp. 1321-1331.

108. Schmidt, J. W.: Funda,entals of Digital Simulation Modelin g. 1981 Winter Simulation Conference Proceedings, Vol. 1, T. F. Oren, C. M. Delfosse, and C. M. Shub, eds., IEEE, 1981, pp. 13-21.

TABLE I. - THERMAL DECOMPOSITION TEMPERATURES AND BOND DISSOCIATION ENERGIES FOR VARIOUS COMPOUNDS

Compound	Bonds	E_{DIS},[a] kJ/mole	T_D, °C
Octacosane	C-C	337	350
11-ethyl-11-methyl pentacosane	C -C-C C	314	331
p-quartaerphenyl	φ-φ	432	454
Polyphenyl ether (5P-4E)	φ-O-φ	423	443
p-bis(p-chlorophenoxy) benzene	φ-Cl	419	409
p-bis(p-bromophenoxy) benzene	φ-Br	335	387
Fluorinated polyether	CF_3-CF_3	406	390
Synthetic paraffinic	C-C	337	314
Alkylated benzene	φ-C-CH	335	340

[a]From ref. 21.

TABLE II. - OXIDIZABILITY OF VARIOUS ORGANIC COMPOUNDS

[From ref. 60.]

Substrate	$k_p/(2k_t)^{1/2} \times 10^3 (M^{-1/2} sec^{-1/2})$
2,3-Dimethyl-2-butene	3.2
Cyclohexene	2.3
1-Octene	.06
Cumene	1.5
Ethylbenzene	.21
Toluene	.01
p-Xylene	.05
Benaldehyde	290
Benzyl alcohol	.85
2,4,6-Trimethylheptane	.09

TABLE III. - X-H BOND ENERGIES

[From ref. 57.]

Compound	Energy, kcal/mol
CH_3-H	103
n-C_3H_7-H	99
i-C_3H_7-H	94
t-C_4H_9-H	90
CH_2=CH-H	105
C_6H_5-H	103
CH_2=CH-CH_2-H	85
$PhCH_2$-H	85
RCO-H	86
CH_3S-H	88
CH_3PH-H	85
PhO-H	88
PhNH-H	80
ROO-H	90

TABLE IV. - RATE CONSTANTS PER LABILE HYDROGEN FOR REACTION OF SUBSTRATES WITH THEIR OWN PEROXY RADICALS (k_p) AND WITH tert- BUTYLPEROXY RADICALS (k_p') at 30° C

[From ref. 57.]

Substrate	k_p ($M^{-1}sec^{-1}$)	k_p ($M^{-1}sec^{-1}$)	k_p/k_p'
1-Octene	0.5	0.084	6.0
Cyclohexene	1.5	.80	1.9
Cyclopentene	1.7	.85	2.0
2,3-Dimethyl-2-butene	1.14	.14	1.0
Toluene	.08	.012	6.7
Ethylbenzene	.65	.10	6.5
Cumene	.18	.22	.9
Tetralin	1.6	.5	3.2
Benzyl ether	7.5	.3	25.0
Benzyl alcohol	2.4	.065	37.0
Benzyl acetate	2.3	.0075	307
Benzyl chloride	1.50	.008	190
Benzyl bromide	.6	.006	100
Benyl cyanide	1.56	.01	156
Benzaldehyde	33 000	.85	40 000

TABLE V. - EFFECTIVENESS OF INHIBITION BY VARIOUS PHENOLS

[From ref. 25.]

Phenol	0.027
2-Methylphenol	.17
4-t-Butylphenol	.05
4-Methylphenol	.095
2-t-Butylphenol	.26
2,5-Dimethylphenol	.314
2,4-Di-t-butylphenol	.465
2,4,6-Tri-t-butylphenol	.47
2-Methyl-4-t-butylphenol	.515
2,6-Di-t-butyl-4-methylphenol	.65
2,4,6-Trimethylphenol	1.00
2,4-Di-t-butyl-6-methylphenol	1.05

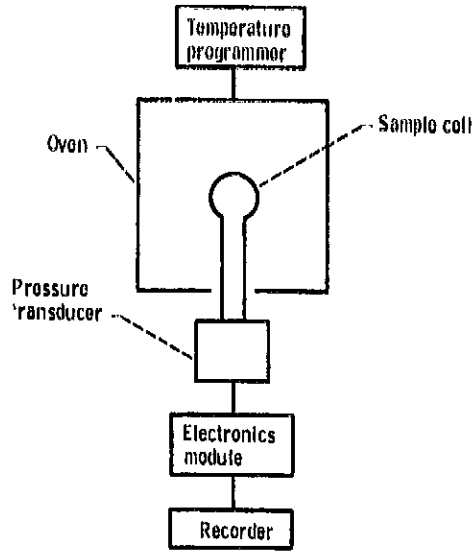

Figure 1. - Recording tensimeter.

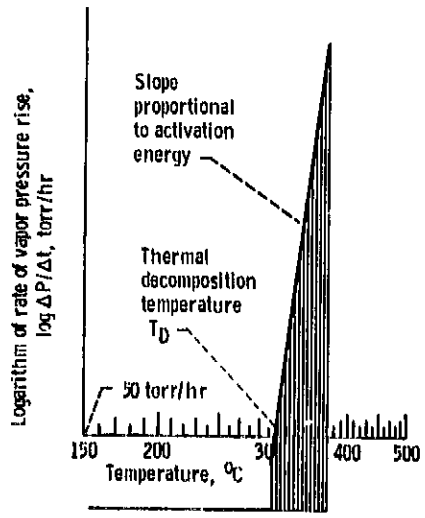

Figure 2. - Typical thermal decomposition curve for synthetic hydrocarbon. Heating interval, 5° C.

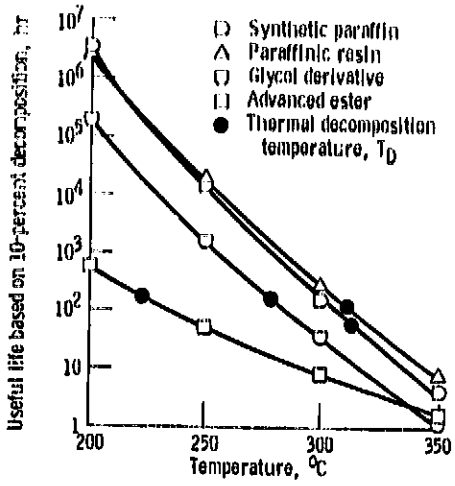

Figure 3. - Useful life (based on 10-percent decomposition) of four lubricants in nitrogen as function of temperature (ref. 15).

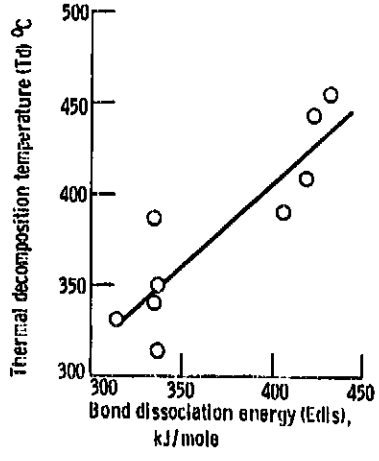

Figure 4. - Thermal decomposition temperature (T_d) as a function of bond dissociation energy (Edis).

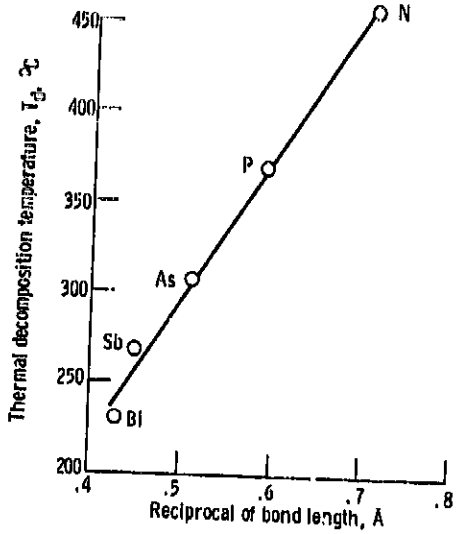

Figure 5. - Thermal decomposition temperature (T_d) as a function of the reciprocal bond length for a series of group V aromatic compounds of the type $(C_6H_5)_nM$ (ref. 12).

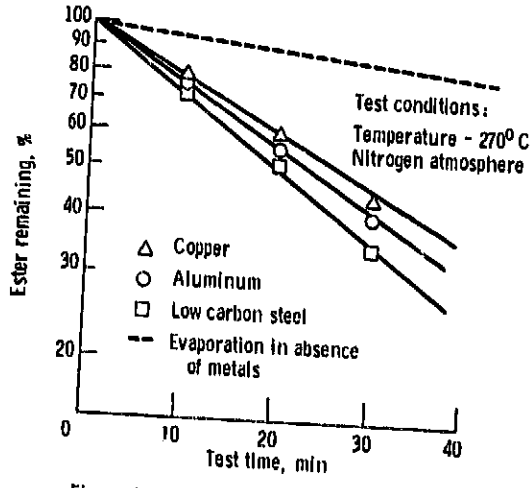

Figure 6. - Time-concentration relationship of diethylhexyl sebacate in evaporation test at 270° C (ref. 23).

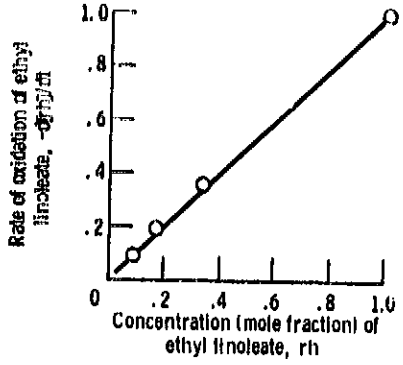

Figure 7. - Oxidation rate as a function of concentration for ethyl linoleate (ref. 25).

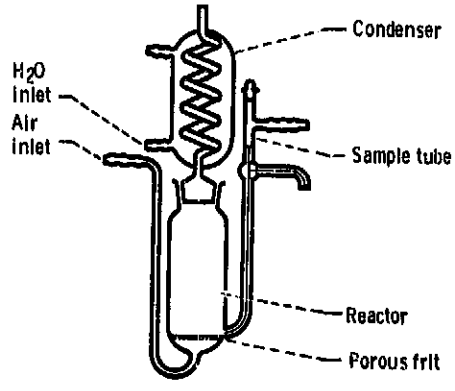

Figure 8. - Typical macro-oxidation cell (ref. 25).

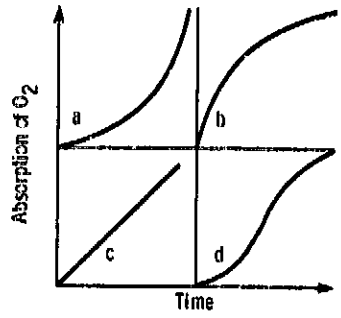

Figure 9. - Types of kinetic curves of the absorption of oxygen (ref. 25).

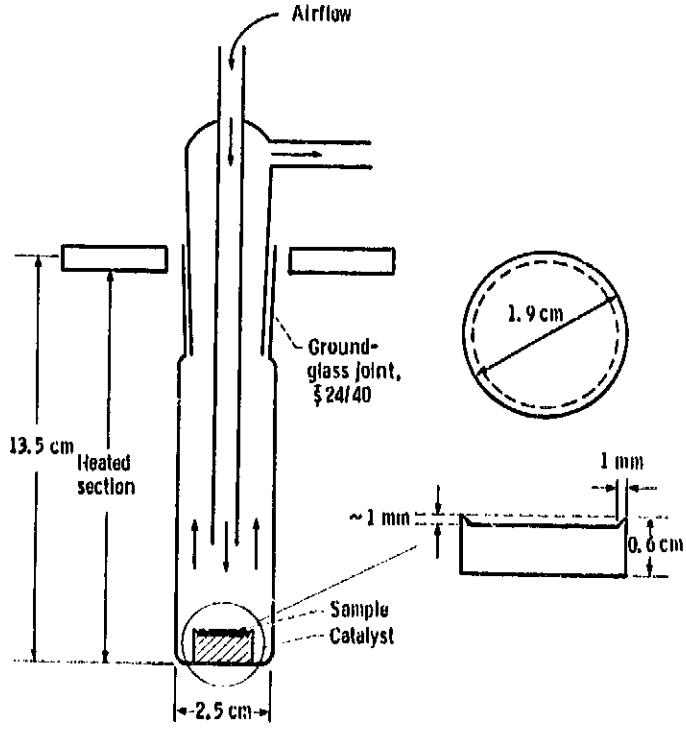

Figure 10. - Micro-oxidation apparatus (refs. 30 and 66).

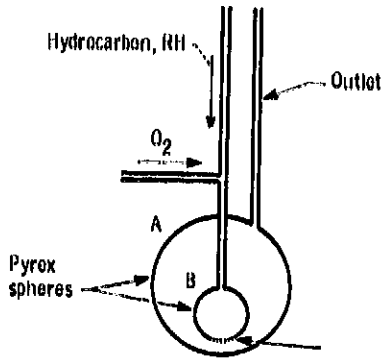

Figure 11. - Stirred flow microreactor (ref. 34).

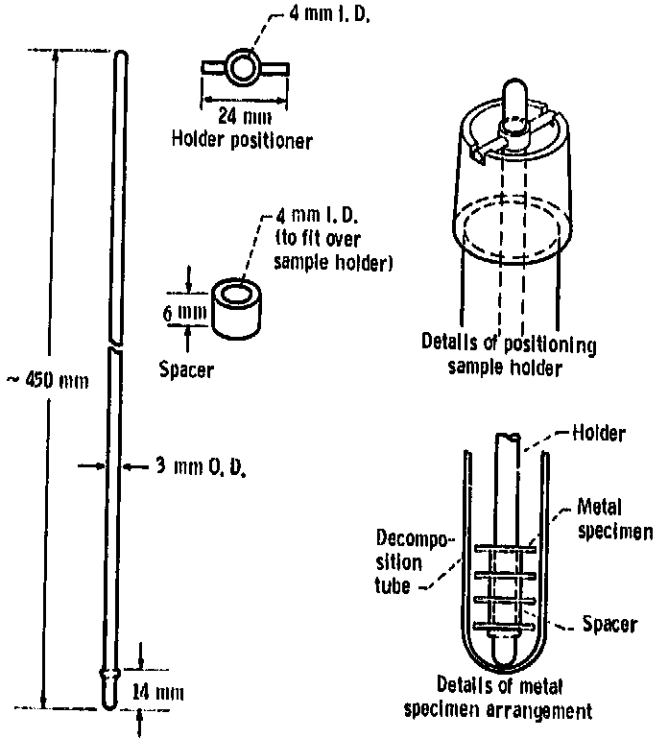

Figure 12. - Thermal oxidative decomposition tube.

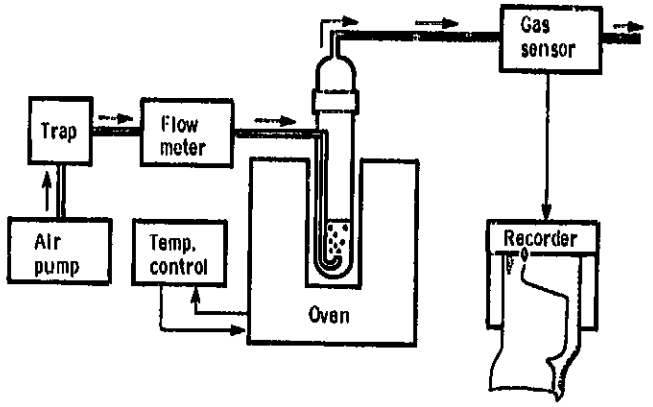

Figure 13. - Oxidative degradation apparatus using an electronic gas sensor (ref. 72).

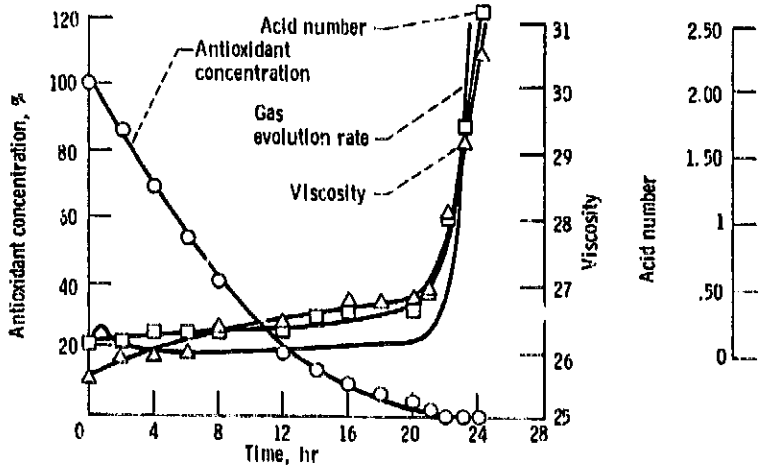

Figure 14. - Acid number, viscosity, antioxidant concentration, and gas evolution as a function of time (pentaerythritol tetrahexanoate, 200° C) (ref. 72).

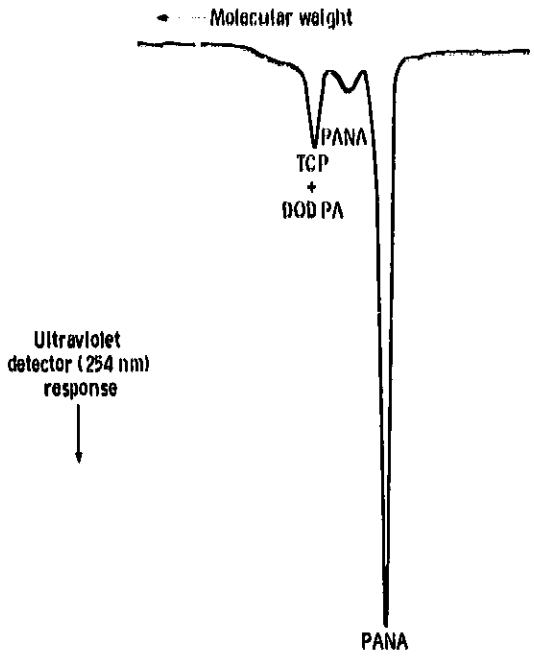

(a) Ultraviolet detector.

Figure 15. - Size exclusion chromatogram of an unused formulated ester (G-mil-99)(ref. 74).

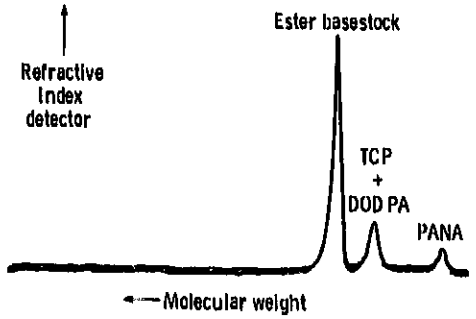

(b) Refractive index detector.

Figure 15. - Concluded.

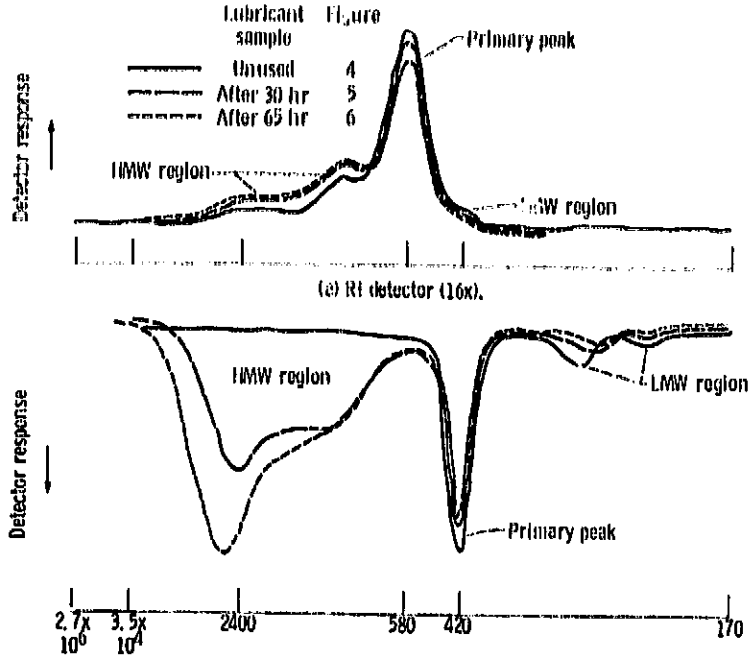

Figure 16. - Summary of size exclusion chromatograms for unused 30- and 65-hr samples (ref. 68).

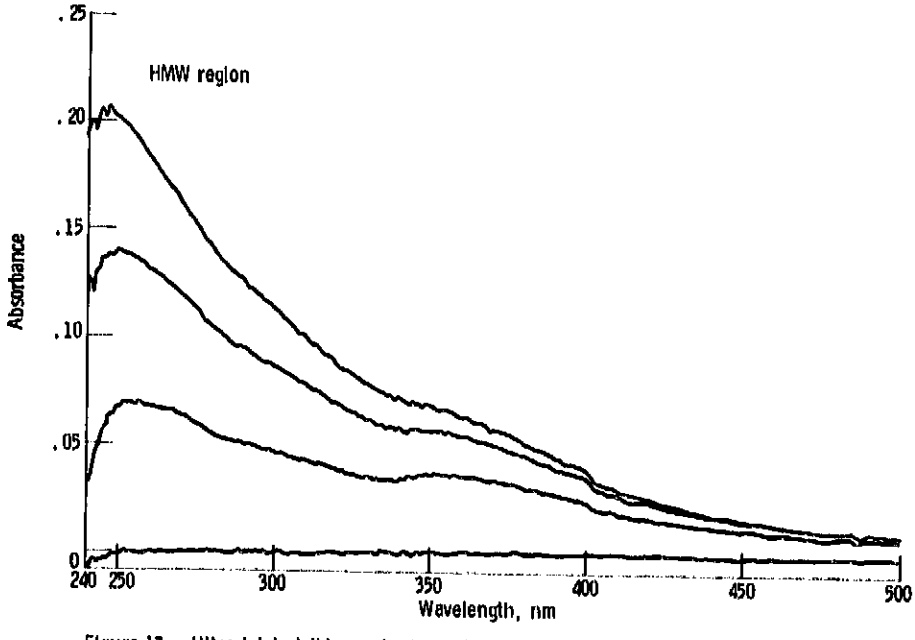

Figure 17. - Ultraviolet-visible spectra from size exclusion separation of oxidized ester (65-hr sample).

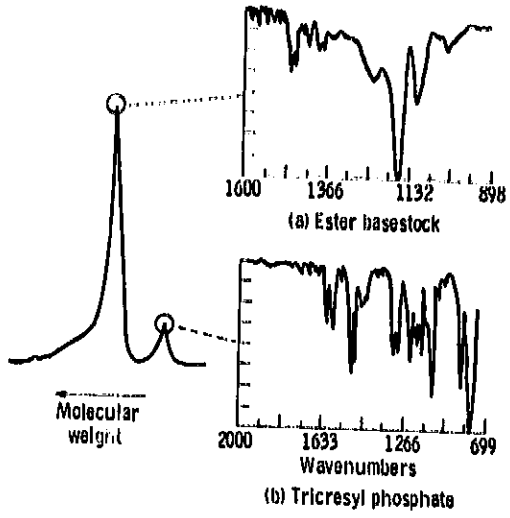

Figure 18. - Infrared spectra of oxidized ester separated by size exclusion chromatography.

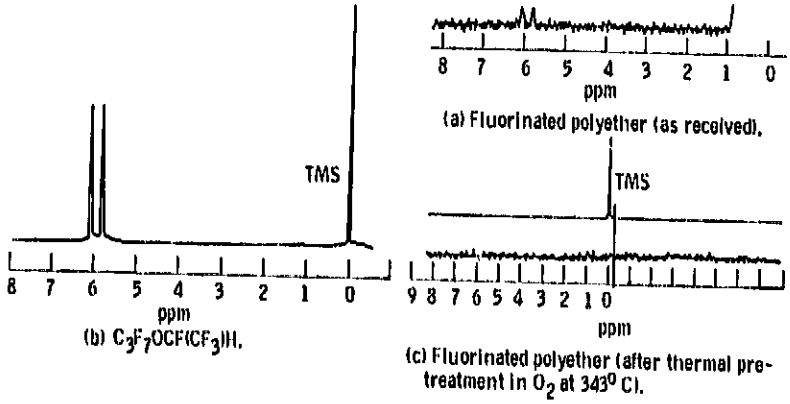

Figure 19. - Proton NMR spectra, referenced to tetramethyl silane (TMS) (ref. 53).

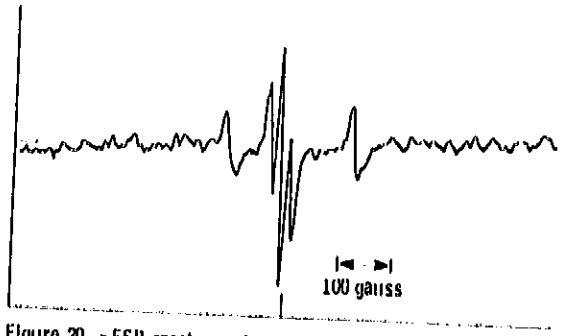

Figure 20. - ESR spectrum of a three-ring thioether from an electrochemical cell.

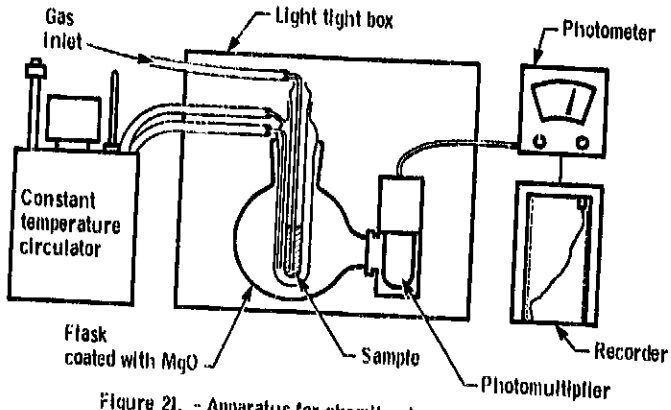

Figure 21. - Apparatus for chemiluminescence studies.

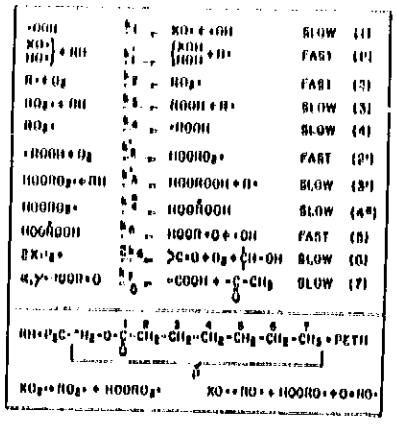

Figure 22. - Reaction scheme for the autoxidation of PETH (ref. 36).

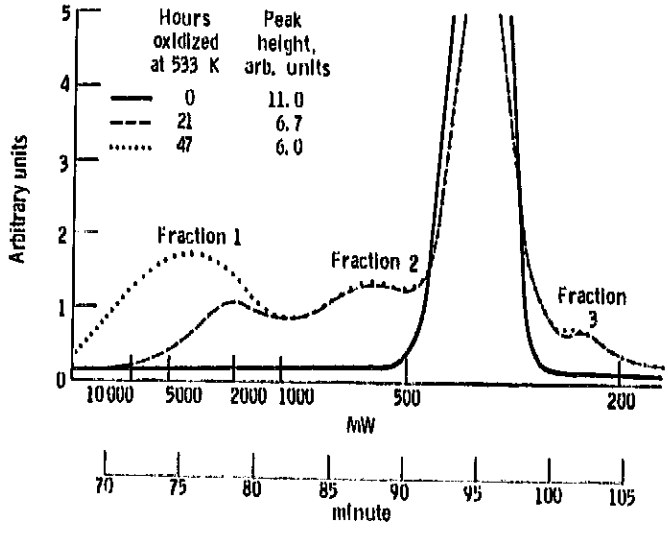

Figure 23. - Gel permeation chromatograms obtained for oxidized di-2-ethylhexylsebacate, no catalyst (ref. 87).

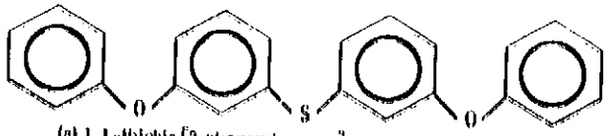

(a) 1, 1'-thiobis [3-phenoxybenzene]; molecular weight, 370.

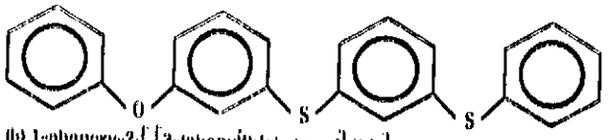

(b) 1-phenoxy-3-{ [3-phenylthio) phenyl] thio] benzene; molecular weight, 386.

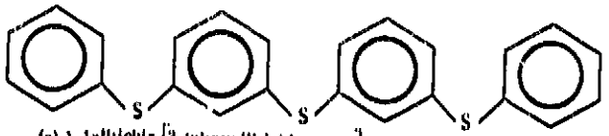

(c) 1, 1'-thiobis [3-phenylthio) benzene]; molecular weight, 402.

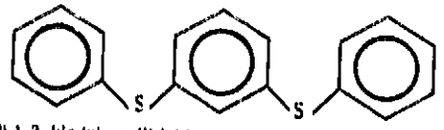

(d) 1, 3-bis (phenylthio) benzene; molecular weight, 294.

Figure 24. - Chemical components of C-ether base fluid (ref. 99).

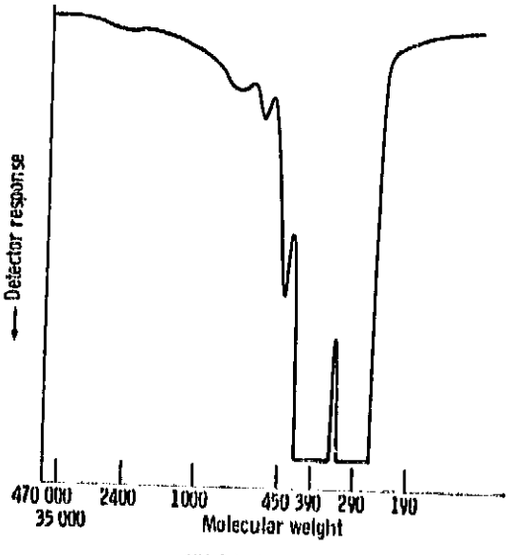

Figure 25. - Gel-permeation chromatogram of a C-ether from micro-oxidation test - catalyst, M-50 steel; test atmosphere, dry air (ref. 56).

$$C_3F_7O(\underset{\displaystyle CF_3}{\underset{|}{CF}}CF_2O)_nR_f$$

(a) Hexafluoropropylene oxide (HFPO) based branched fluids.

$$R_fO(CF_2CF_2O)_m(CF_2O)_nR_f$$

(b) Unbranched perfluoroalkylether fluids.

Figure 26. - Chemical structures of perfluoroalkylether fluids (R_f = CF_3 or C_2F_5).

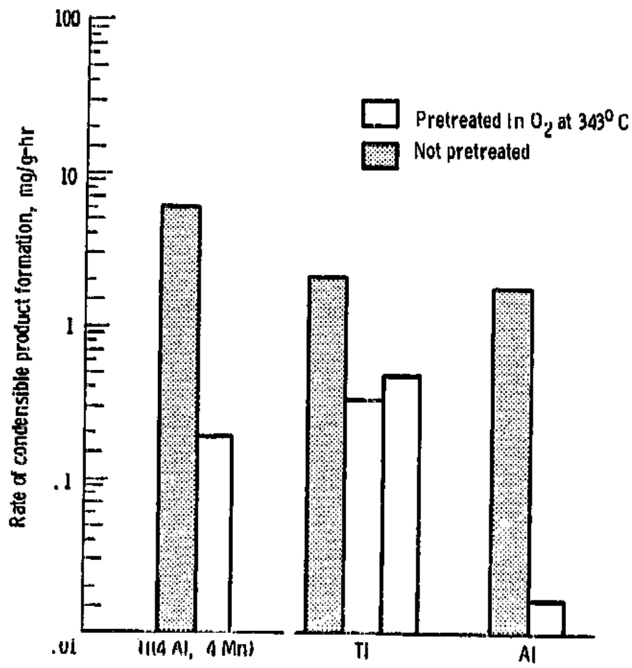

Figure 27. - Effect of metals on degradation of branched perfluoroalkylether 316° C, O_2, 24 hr (ref. 53).

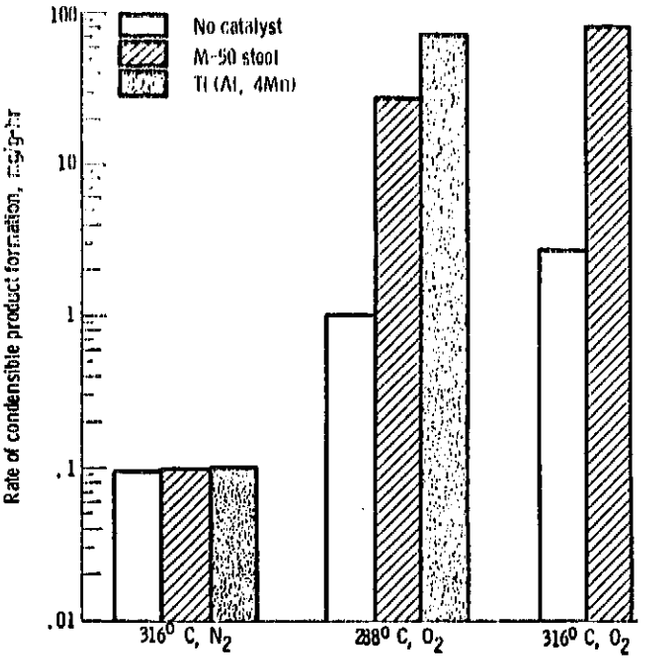

Figure 28. - Rates of condensible product formation for unbranched fluoroalkylether in the presence of metal alloys (ref. 52).

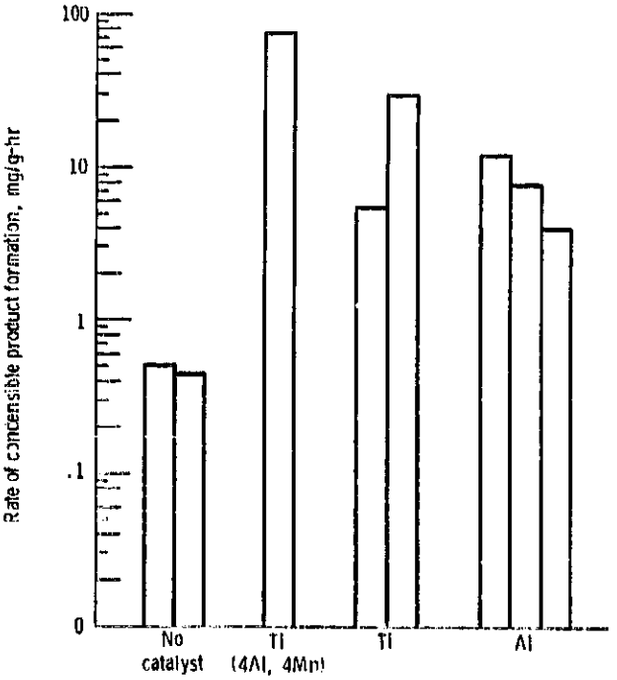

Figure 29. - Effect of metals on the degradation of an unbranched perfluoroalkyl ether (288° C, O_2) (ref. 53).

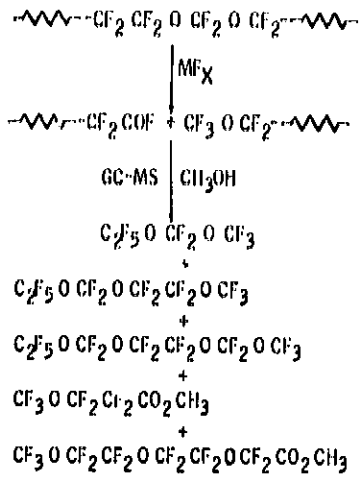

Figure 30. - Degradation of unbranched perfluoralkyl ethers in the presence of Ti (4 Al, 4 Mn) at 288° C in O_2 (ref. 53).

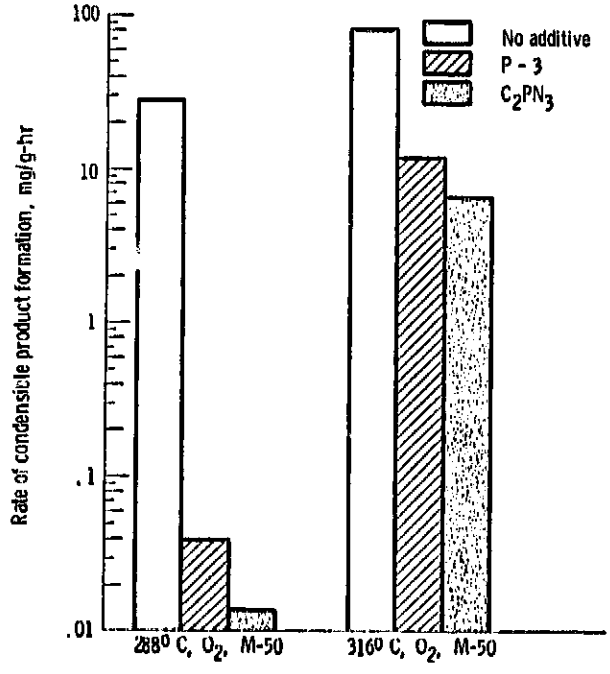

Figure 31. - Effect of degradation inhibitors on the rate of condensible product formation of an unbranched perfluoroalkylether (ref. 52).

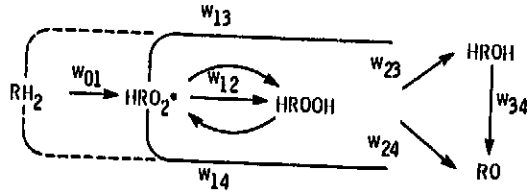

Figure 32 - Carbon-skeleton sequence network of the oxidation of ethylbenzene in the temperature range from 40^0 C to 130^0 C based on the possible mechanism (ref. 107).